Bimodal fission
in the SHF+BCS approach

A. Staszczak
(UMCS, UT, ORNL)

International Workshop
Joint JUSTIPEN-LACM Meeting
Joint Institute for Heavy Ion Research, Oak Ridge, Tennessee, USA
Oak Ridge National Laboratory
March 5-8, 2007

The constrained HF procedure

- The constraints act as the external fields capable to deform the nucleus in different ways
- The collective coordinates can be defined in a natural way by measuring the deformations generated by the various constraints

The constrained mean field theory defines the deformed $\Phi\{q\}$ states (BCS- or HFB-type) that solve the variational equation:

$$\delta\left[\left\langle \Phi\{q\}\right| \hat{H} - \lambda_N \hat{N} - \lambda_Z \hat{Z} + \underbrace{\sum_j \tfrac{1}{2} c_j \left(\hat{Q}_j - \mu_j\right)^2}_{\text{quadratic multipole constraints}} \left|\Phi\{q\}\right\rangle\right] = 0$$

with the constraint conditions

$$\left\langle \Phi\{q\}\right| \hat{N} \left|\Phi\{q\}\right\rangle = N, \quad \left\langle \Phi\{q\}\right| \hat{Z} \left|\Phi\{q\}\right\rangle = Z, \quad \left\langle \Phi\{q\}\right| \hat{Q}_j \left|\Phi\{q\}\right\rangle = q_j.$$

The multipole constraints prescribe different kinds of deformation characterized by the set of parameters $\{q\} = \{q_1, q_2, \ldots, q_N\}$.

$\hat{H}$ is the many-body nuclear (non-relativistic) Hamiltonian

$$\hat{H} = \sum_{i=1}^{A} \frac{\hat{p}_i^2}{2m} - \frac{\left\langle \sum_i \hat{p}_i {}^{2} \right\rangle}{2Am} + \frac{1}{2} \sum_{i \neq j}^{A} \hat{V}_{ij}^{(eff)}$$

center-of-mass "projection" term (in the VAP technique), to eliminate spurious mode associated with the broken translational symmetry

nuclear effective interaction term (Skyrme, Gogne type forces)

To describe the fission process most "important" are the low-multipolarity mass moments, i.e.,

$$\hat{Q}_{20}(\vec{r}) = \sqrt{16\pi/5} \sum_i r_i^2 Y_{20}^*(\theta_i, \phi_i),$$ "nuclear stretching"

$$\hat{Q}_{30}(\vec{r}) = \sqrt{4\pi/7} \sum_i r_i^3 Y_{30}^*(\theta_i, \phi_i),$$ "reflection-asymmetry"

$$\hat{Q}_{40}(\vec{r}) = \sqrt{4\pi/9} \sum_i r_i^4 Y_{40}^*(\theta_i, \phi_i).$$ "necking"

Seniority pairing:

J. Dudek, *et al.*, J. Phys. **G6**(1980)447.

$$G^n A = \begin{cases} 18.95 - 0.078 \; N-Z \;, & Z < 88 \\ 19.3 \; - 0.084 \; N-Z \;, & Z \geq 88 \end{cases}$$

$$G^p A = \begin{cases} 17.90 + 0.176 \; N-Z \;, & Z < 88 \\ 13.3 \; + 0.217 \; N-Z \;, & Z \geq 88 \end{cases}$$

$$\tilde{G}^{n/p} = f_{n/p} G^{n/p}$$

In pairing (BCS) window N (or Z) s. p. states are taken,

$f_{n/p}$ parameter is chosen to reproduce $\Delta_{n/p}$ for ^{252}Fm.

$f_n = 1.28$, $f_p = 1.11$

Size of the basis

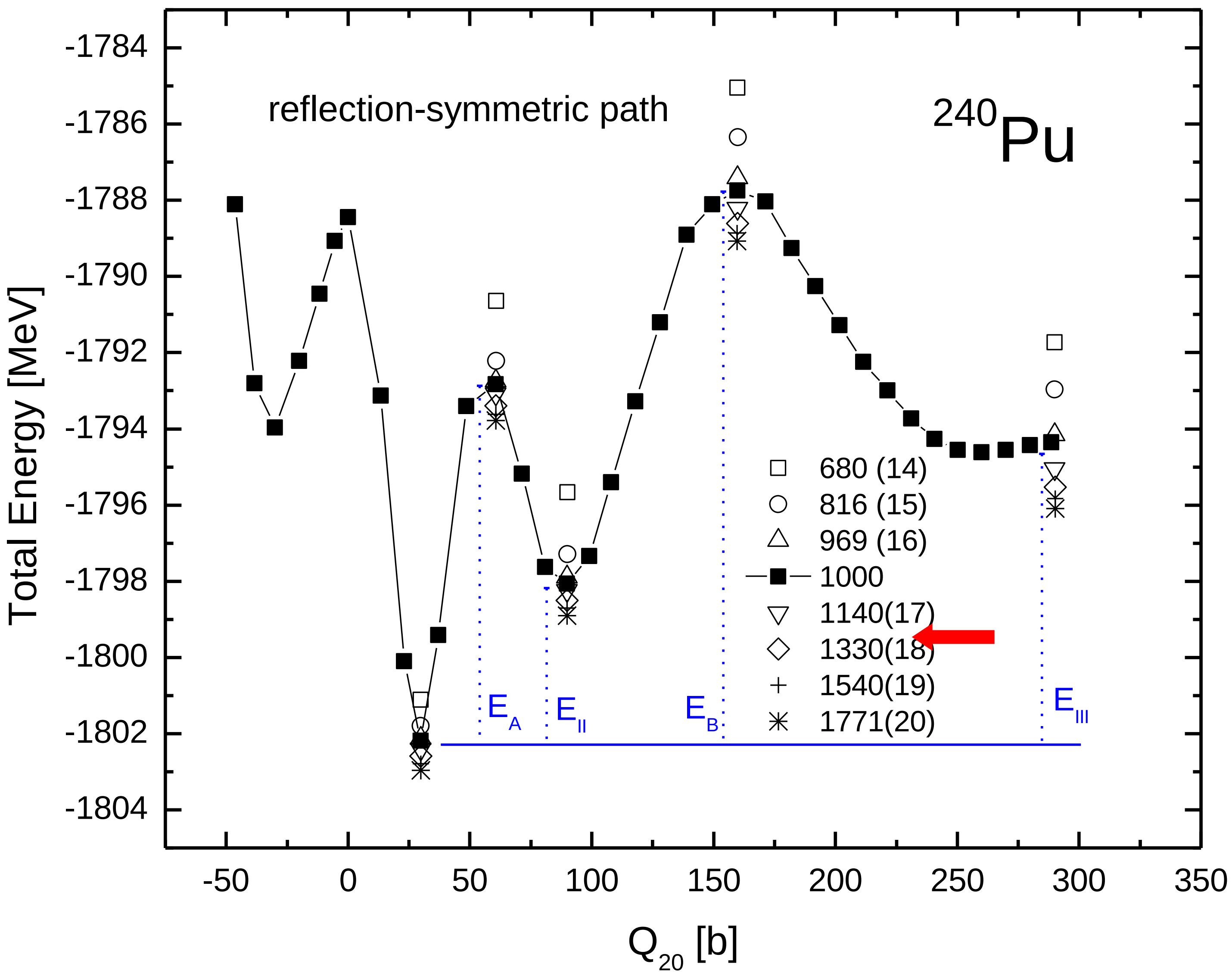

1140 s. p. states of deformed 3D h. o.

SYMMETRIC BIMODAL FISSION

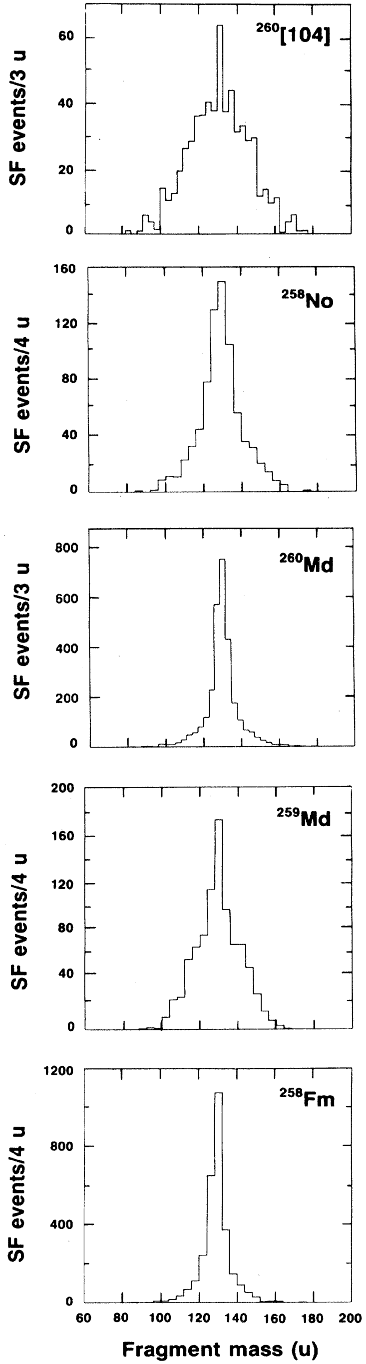

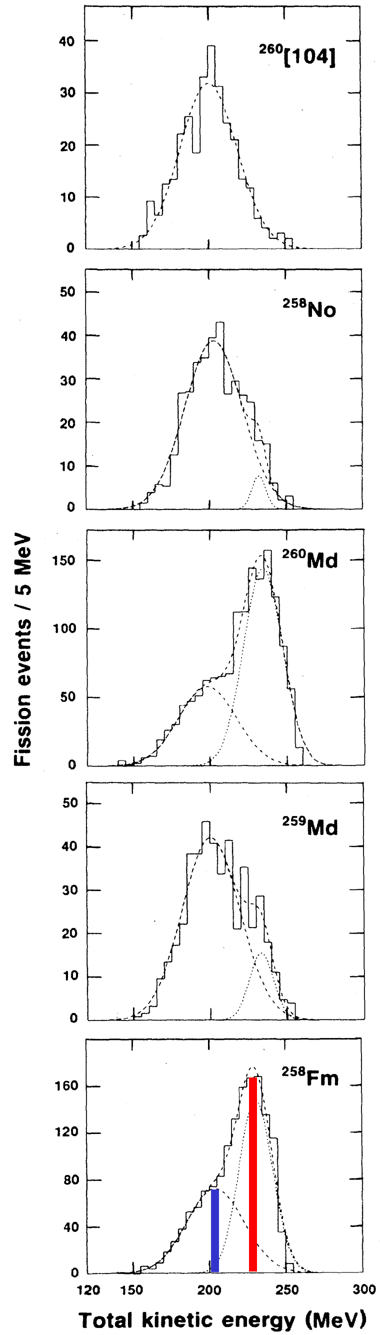

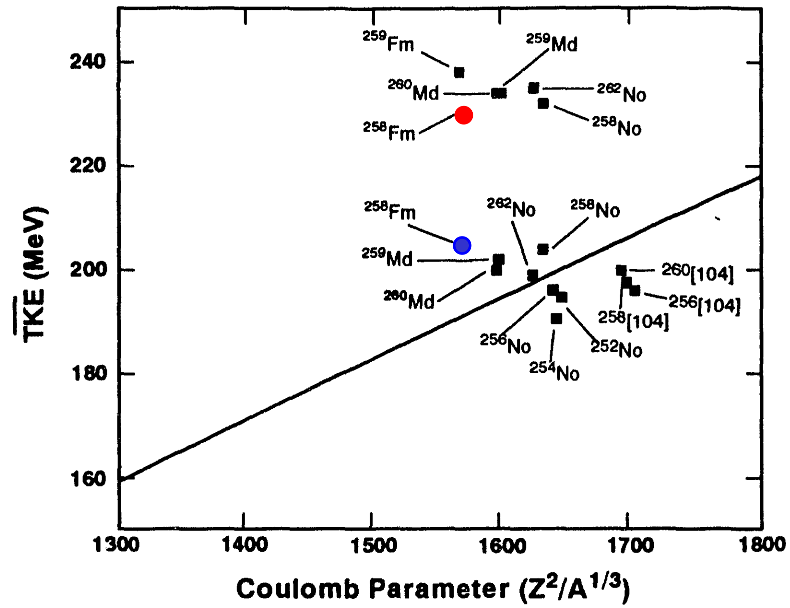

Fig. 7. Comparison of expected liquid-drop TKE's (line) with the TKE's obtained for the nuclides reported here and for the two groups of TKE's found for the bimodal nuclides. The line is defined by the best fit of experimental TKE's to a linear dependency on the Coulomb parameter, $Z^2/A^{1/3}$ in the liquid-drop model of fission.[26]

E.K. Hulet, *et al*.,
Phys. Rev. Lett. **56** (1986) 313,
Phys. Rev. C **40** (1989) 770

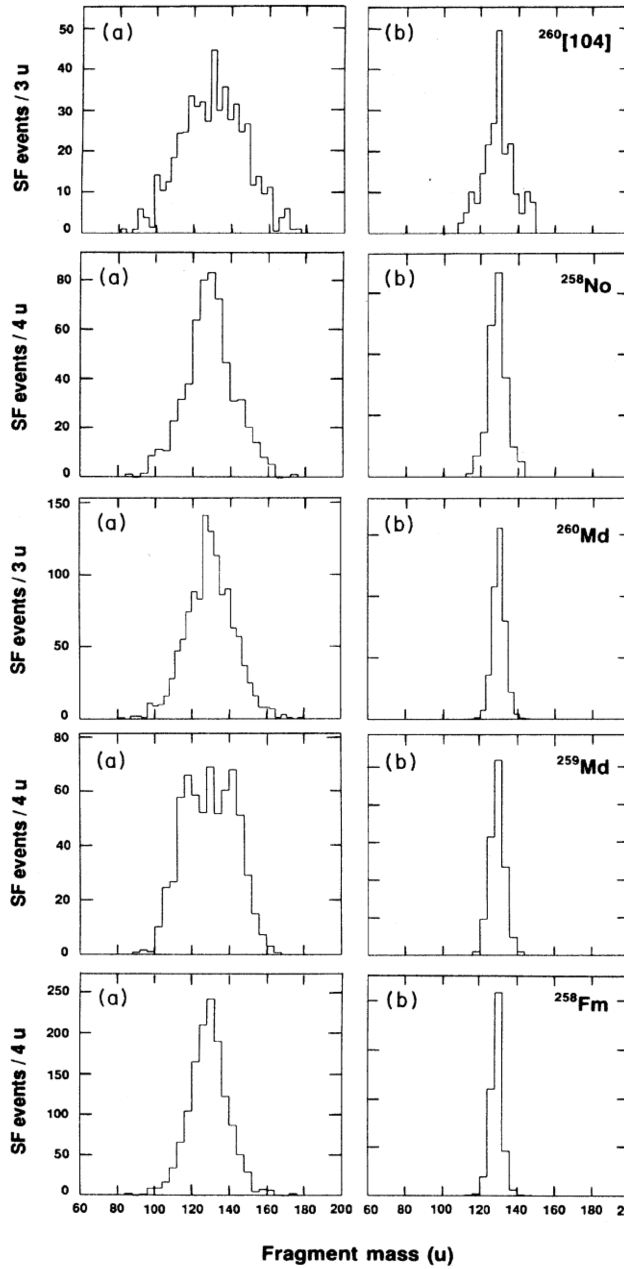

FIG. 8. Mass distributions obtained by sorting fission events according to their total kinetic energies: (a) for events with TKE's < 220 MeV and (b) for those with TKE's ≥ 220 MeV.

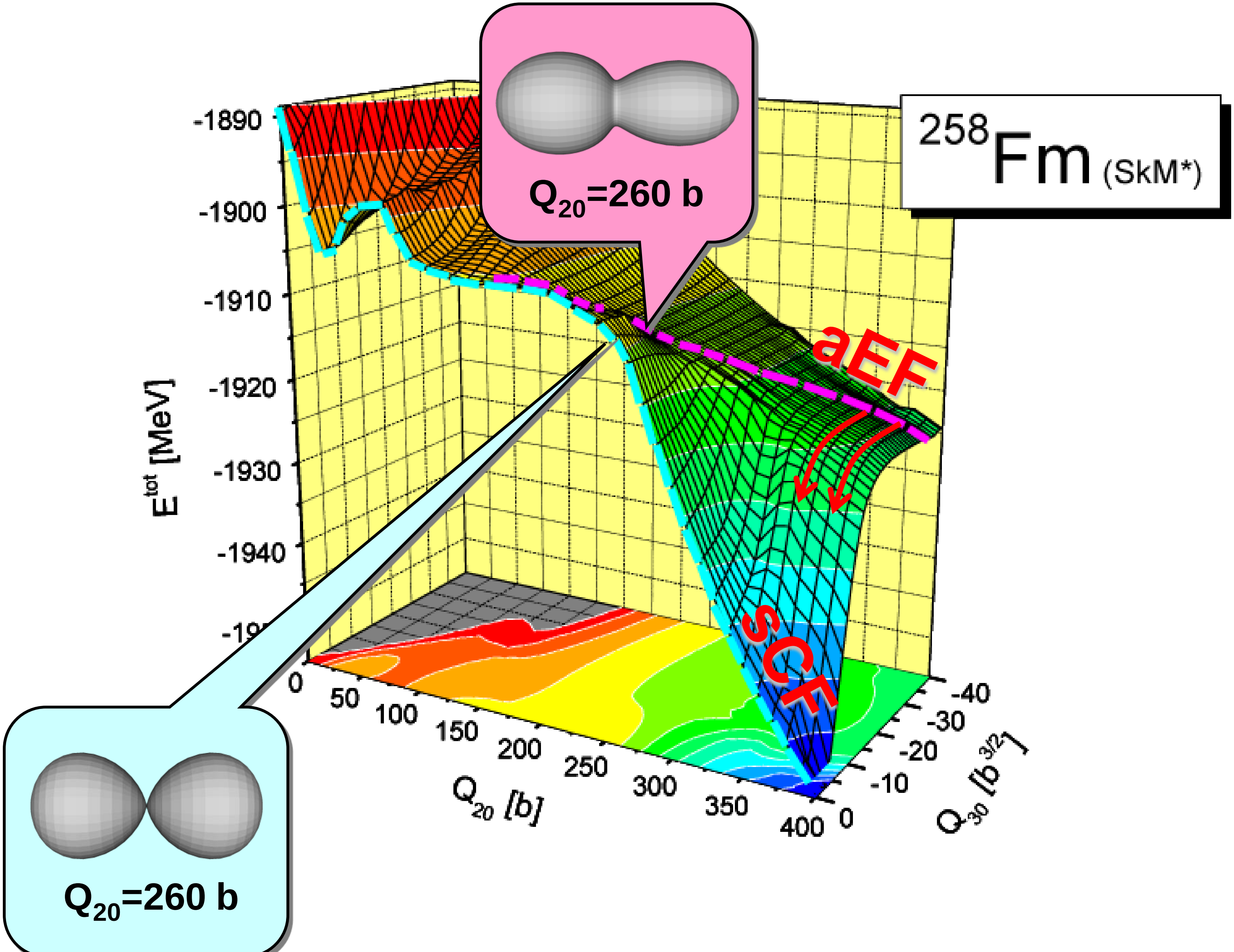

^{258}Fm (SkM*)
Q_{20}=260 b
Q_{20}=260 b
aEF
SCF
E^{tot} [MeV]
-1890
-1900
-1910
-1920
-1930
-1940
Q_{20} [b]
0
50
100
150
200
250
300
350
400
Q_{30} [$b^{3/2}$]
0
-10
-20
-30
-40

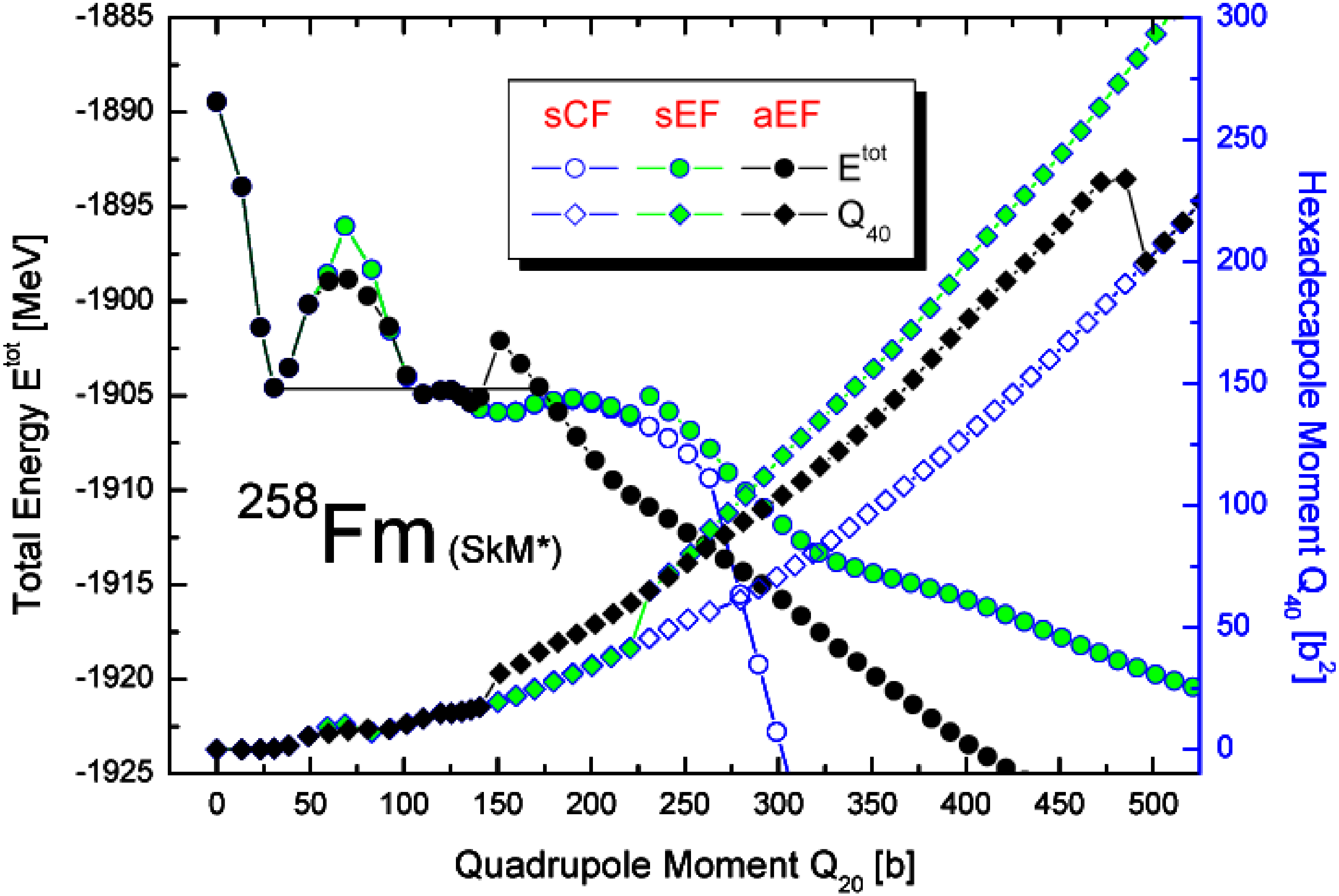
sCF
sEF
aEF
E^tot
Q_40
258Fm (SkM*)
Total Energy E^tot [MeV]
Hexadecapole Moment Q_40 [b^2]
Quadrupole Moment Q_20 [b]
-1885
-1890
-1895
-1900
-1905
-1910
-1915
-1920
-1925
0
50
100
150
200
250
300
350
400
450
500
300
250
200
150
100
50
0

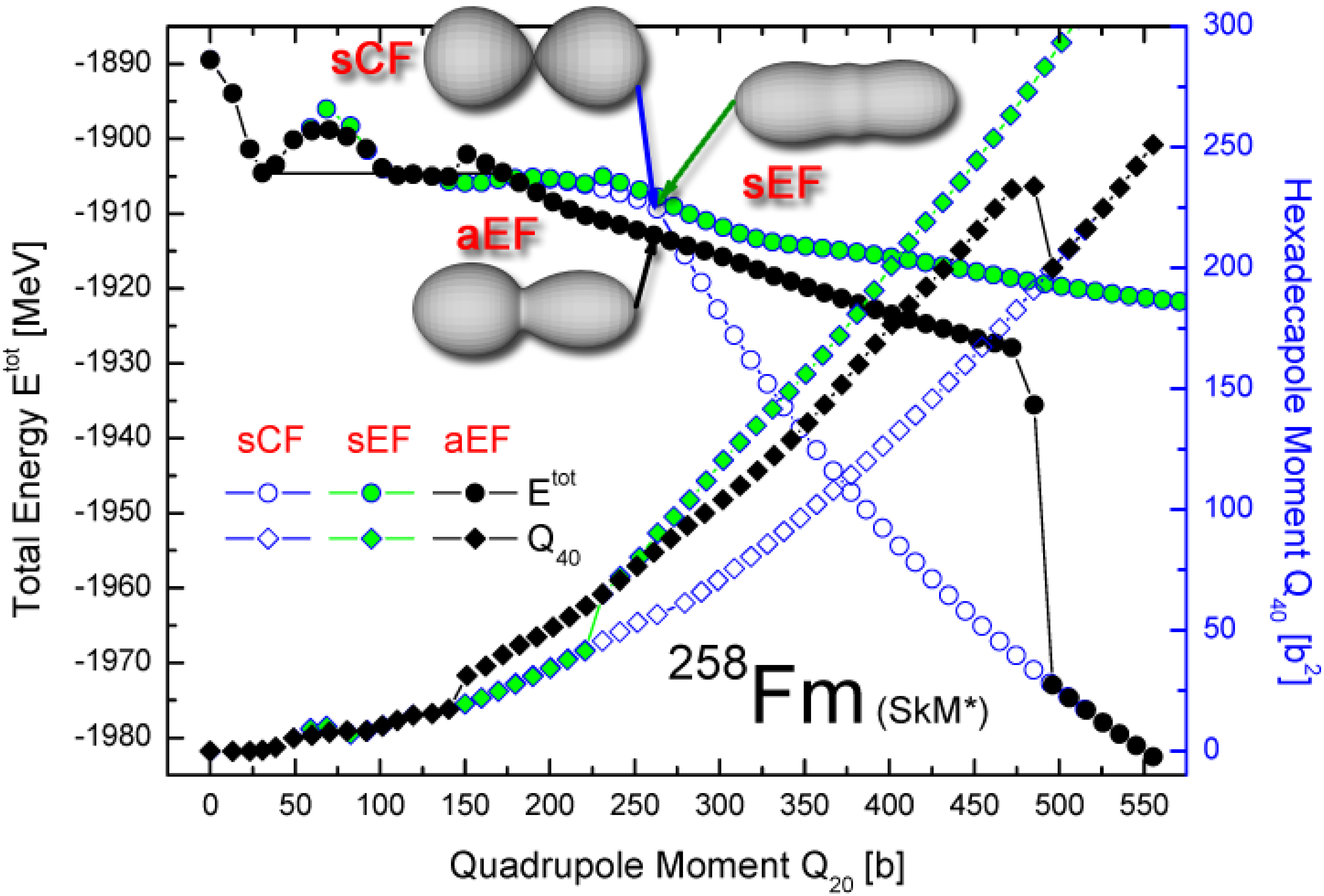

sCF
sEF
aEF
sCF sEF aEF
E^tot
Q40
258Fm (SkM*)
Total Energy E^tot [MeV]
Hexadecapole Moment Q40 [b²]
Quadrupole Moment Q20 [b]

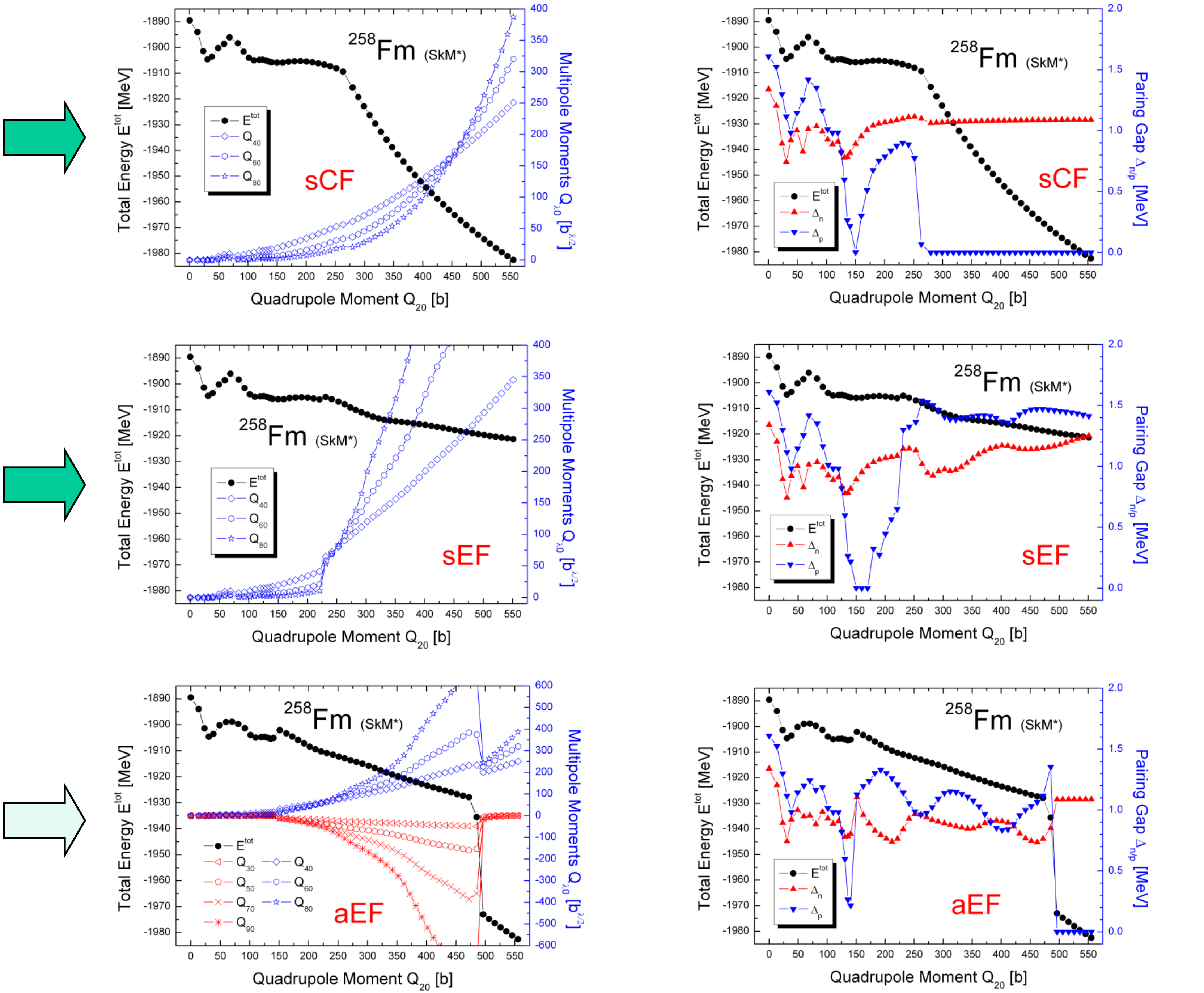

^{258}Fm (SkM*)
sCF
sEF
aEF
Total Energy E^{tot} [MeV]
Quadrupole Moment Q_{20} [b]
Multipole Moments $Q_{\lambda 0}$ [$b^{\lambda/2}$]
Paring Gap $\Delta_{n/p}$ [MeV]
E^{tot}
Q_{30}
Q_{40}
Q_{50}
Q_{60}
Q_{70}
Q_{80}
Q_{90}
Δ_n
Δ_p

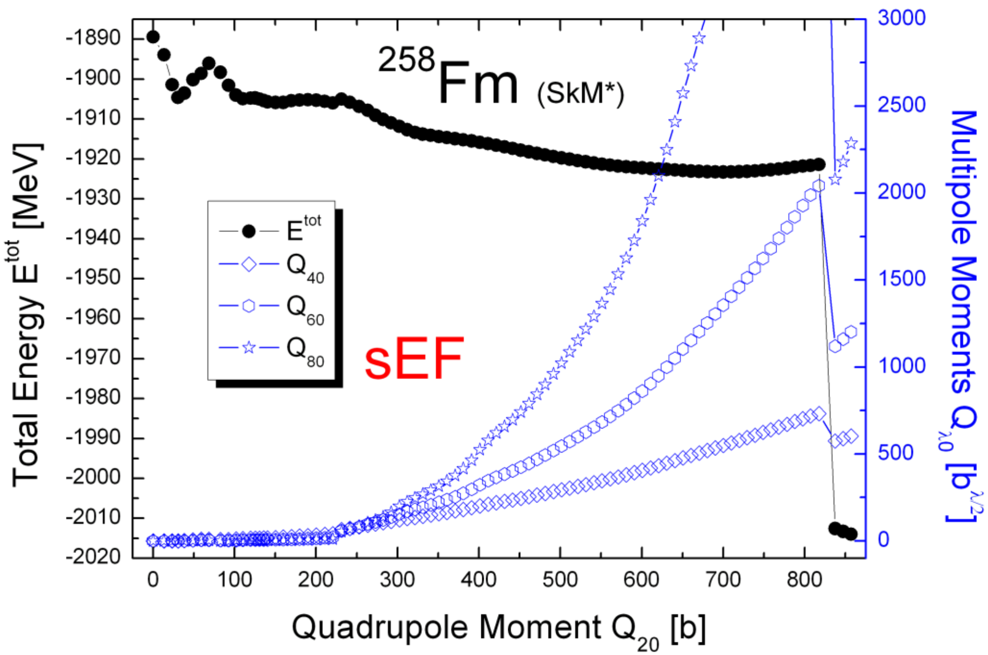

258Fm (SkM*)
sEF
Total Energy E^tot [MeV]
Multipole Moments Q_λ0 [b^λ/2]
Quadrupole Moment Q20 [b]
E^tot
Q40
Q60
Q80

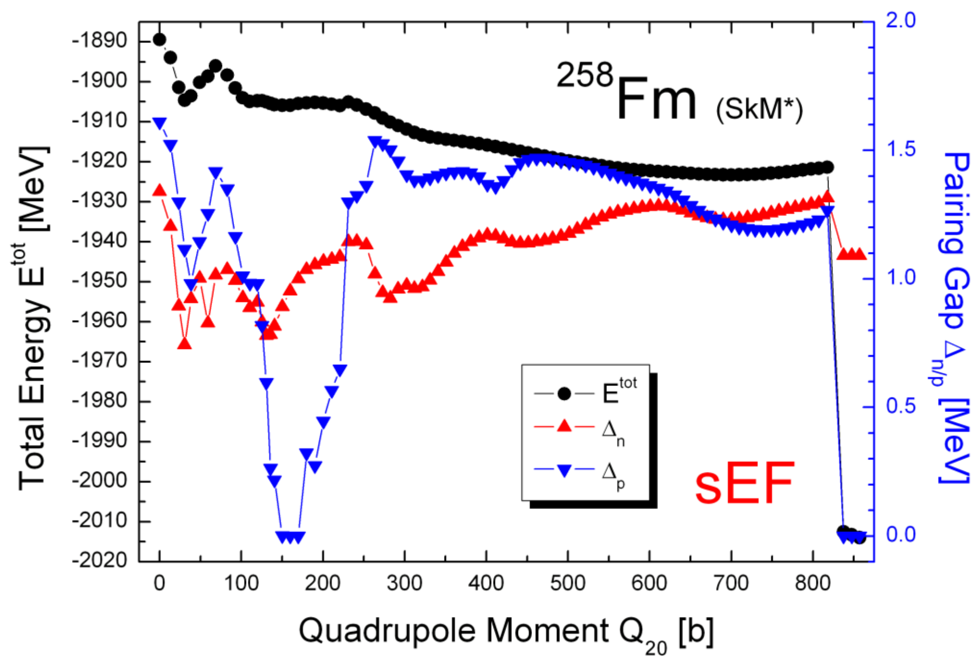

258Fm (SkM*)
sEF
Total Energy E^tot [MeV]
Pairing Gap Δn/p [MeV]
Quadrupole Moment Q20 [b]
E^tot
Δn
Δp

^{258}Fm (SkM*) sCF

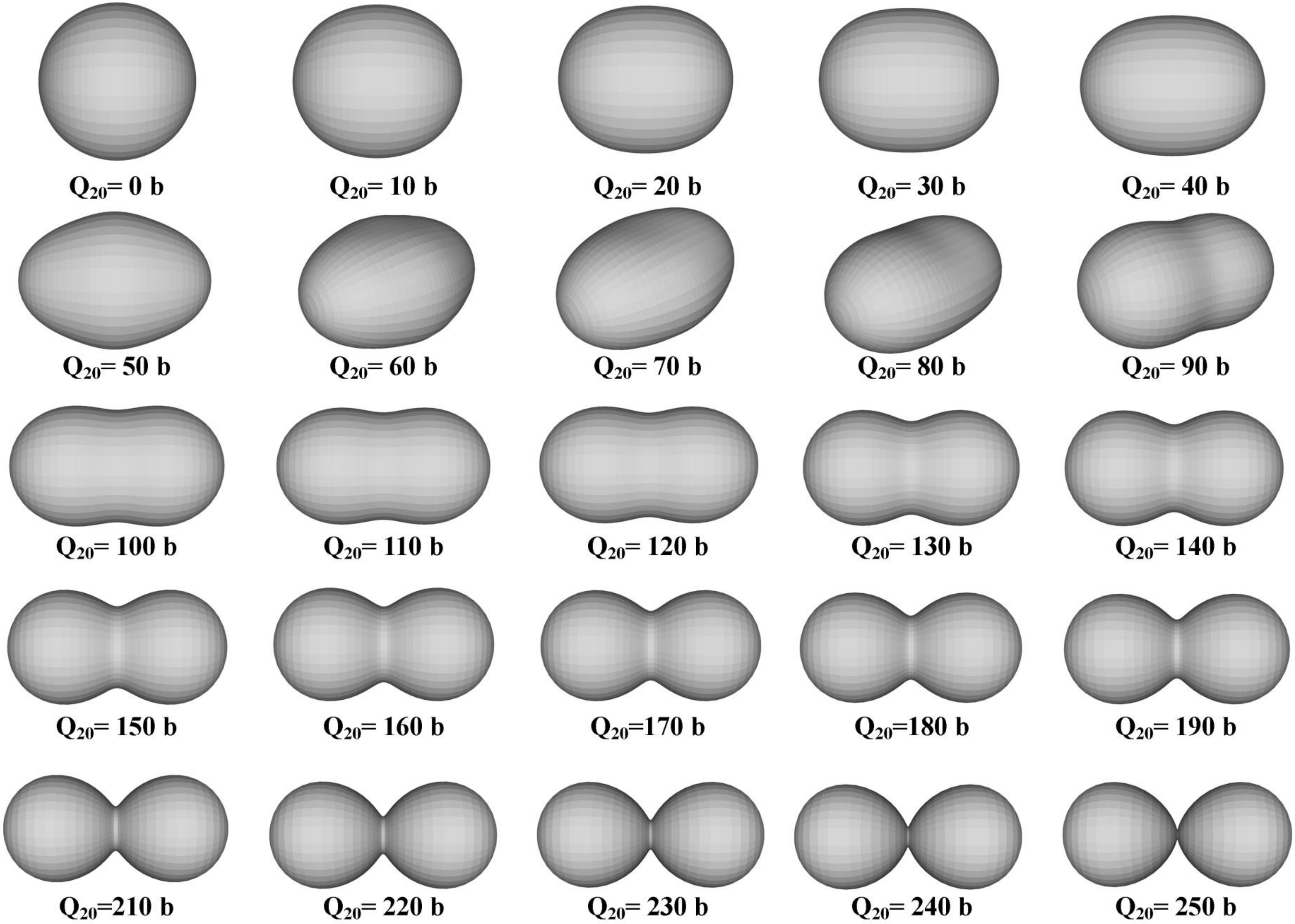

^{258}Fm (SkM*) sEF

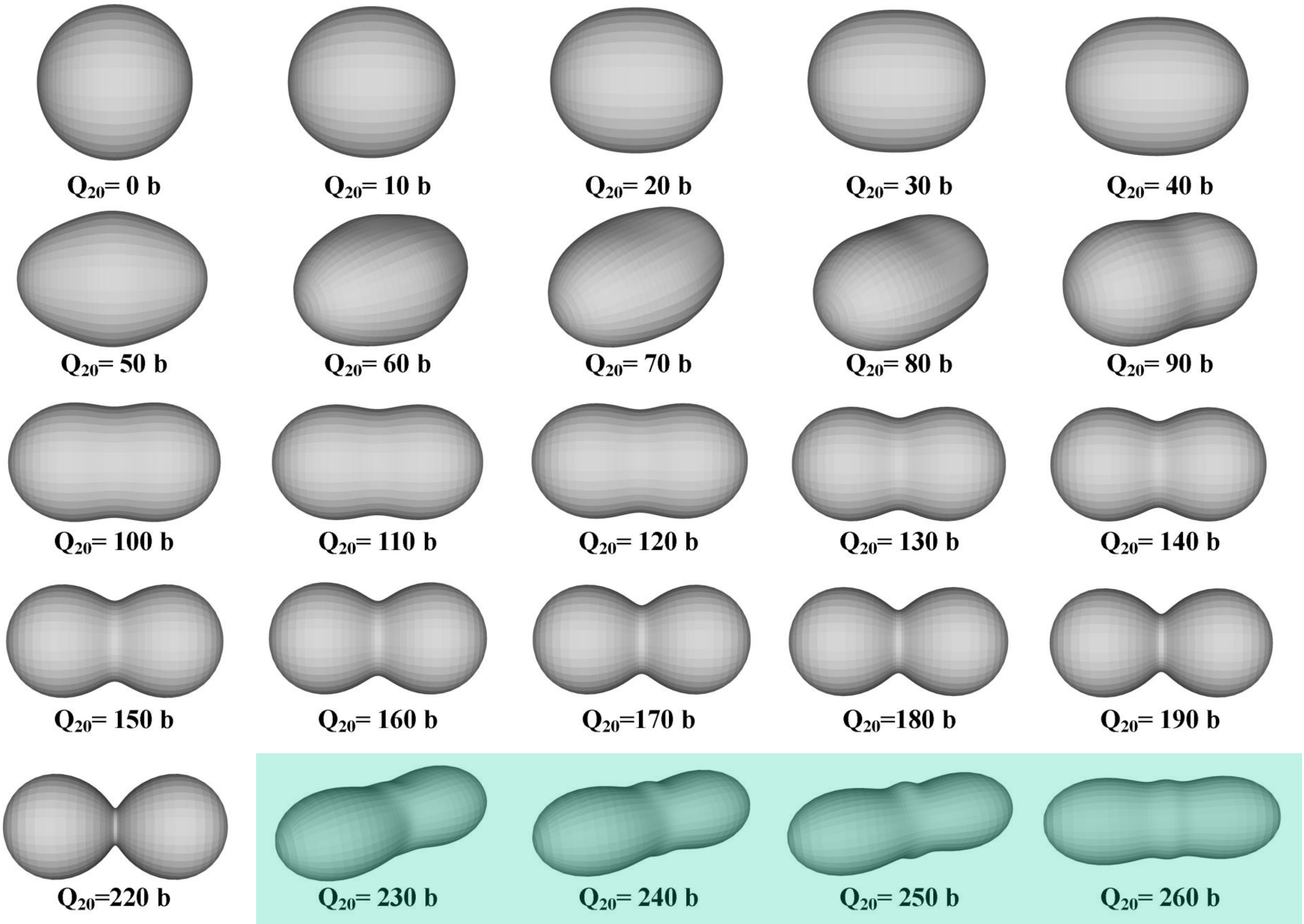

^{258}Fm (SkM*) aEF

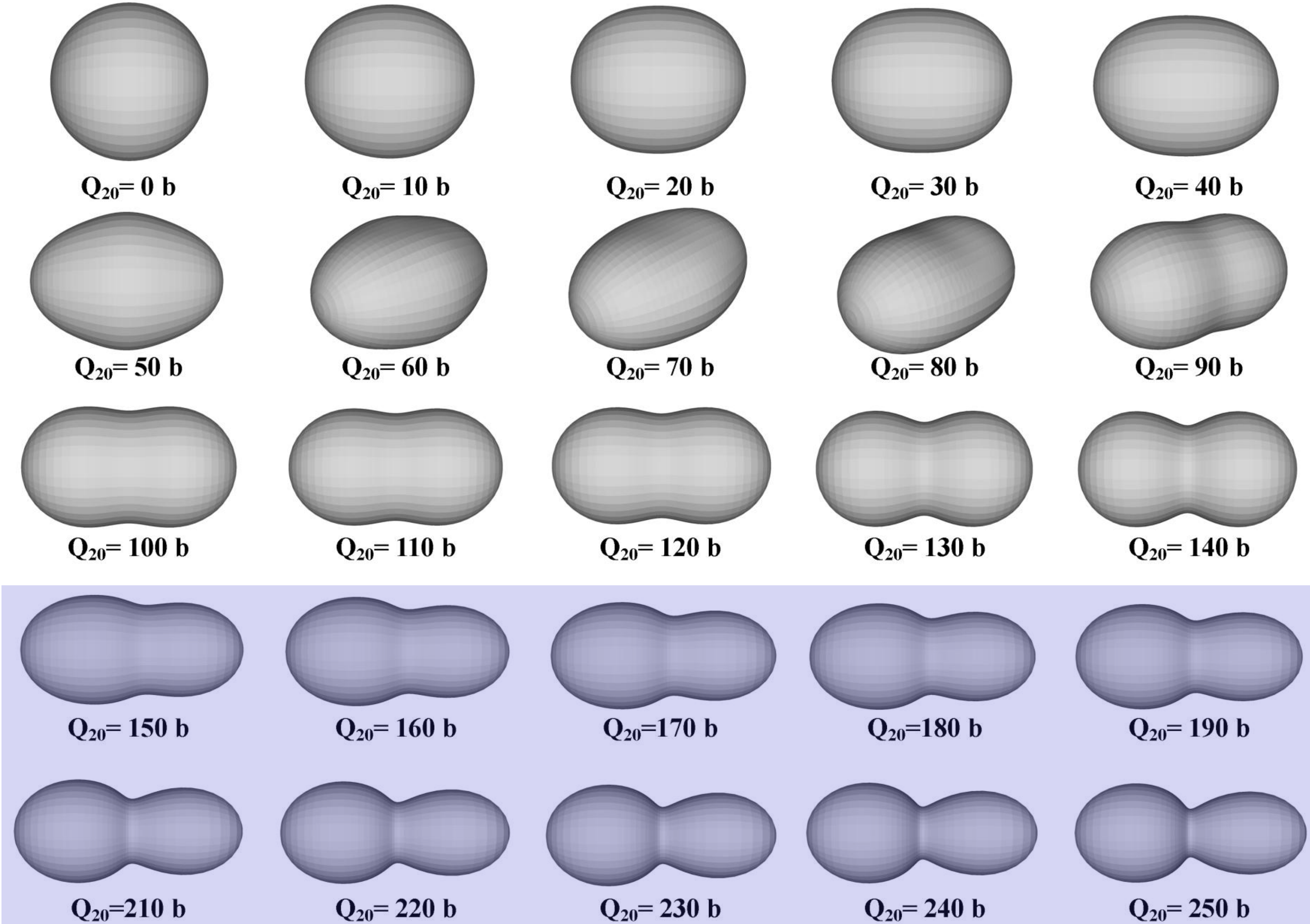

^{258}Fm

"triple-mod" fission
(sCF, sEF & aEF)

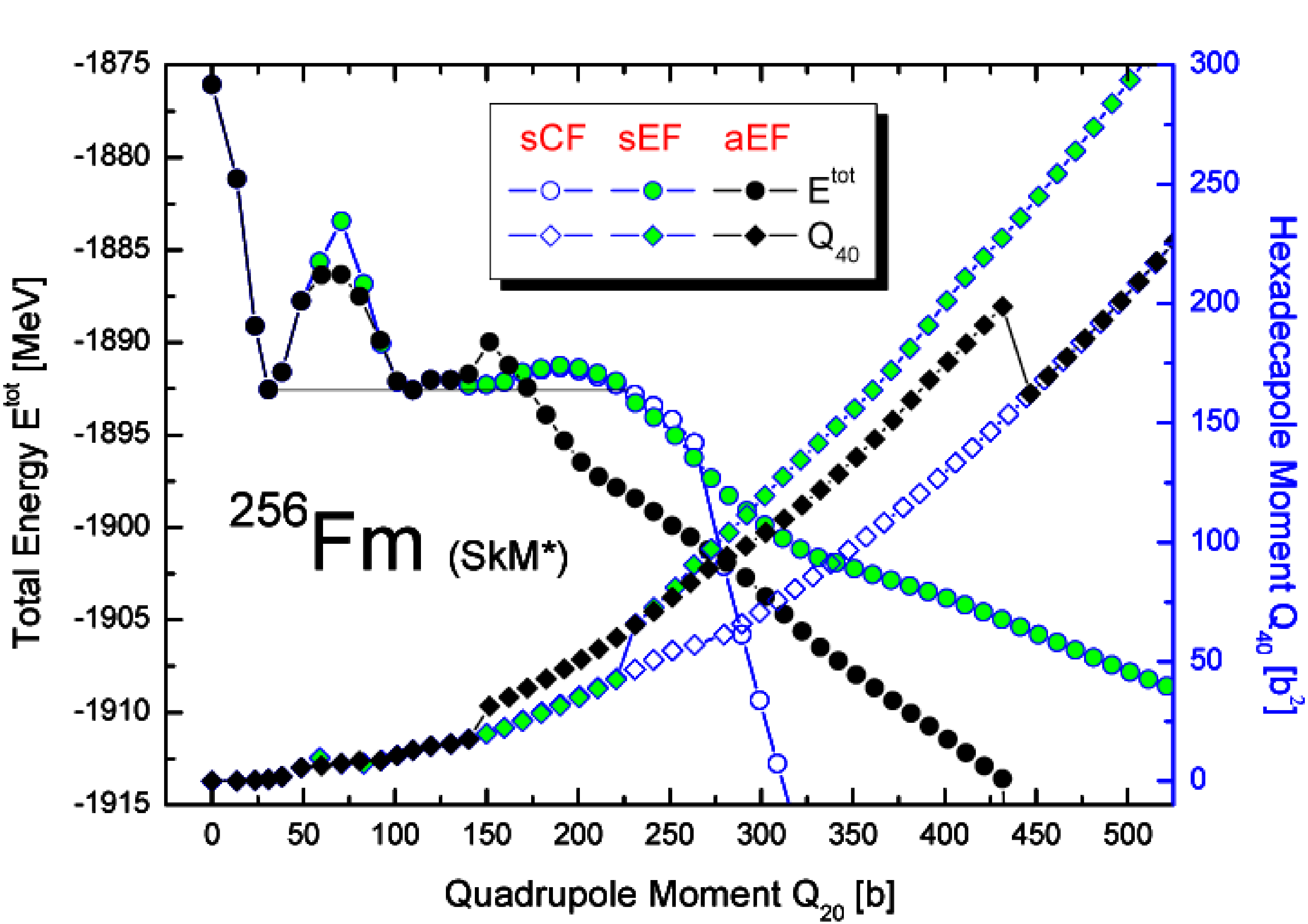

sCF sEF aEF
E^{tot}
Q_{40}
^{256}Fm (SkM*)
Total Energy E^{tot} [MeV]
Hexadecapole Moment Q_{40} [b^2]
Quadrupole Moment Q_{20} [b]
-1875
-1880
-1885
-1890
-1895
-1900
-1905
-1910
-1915
0 50 100 150 200 250 300 350 400 450 500
300 250 200 150 100 50 0

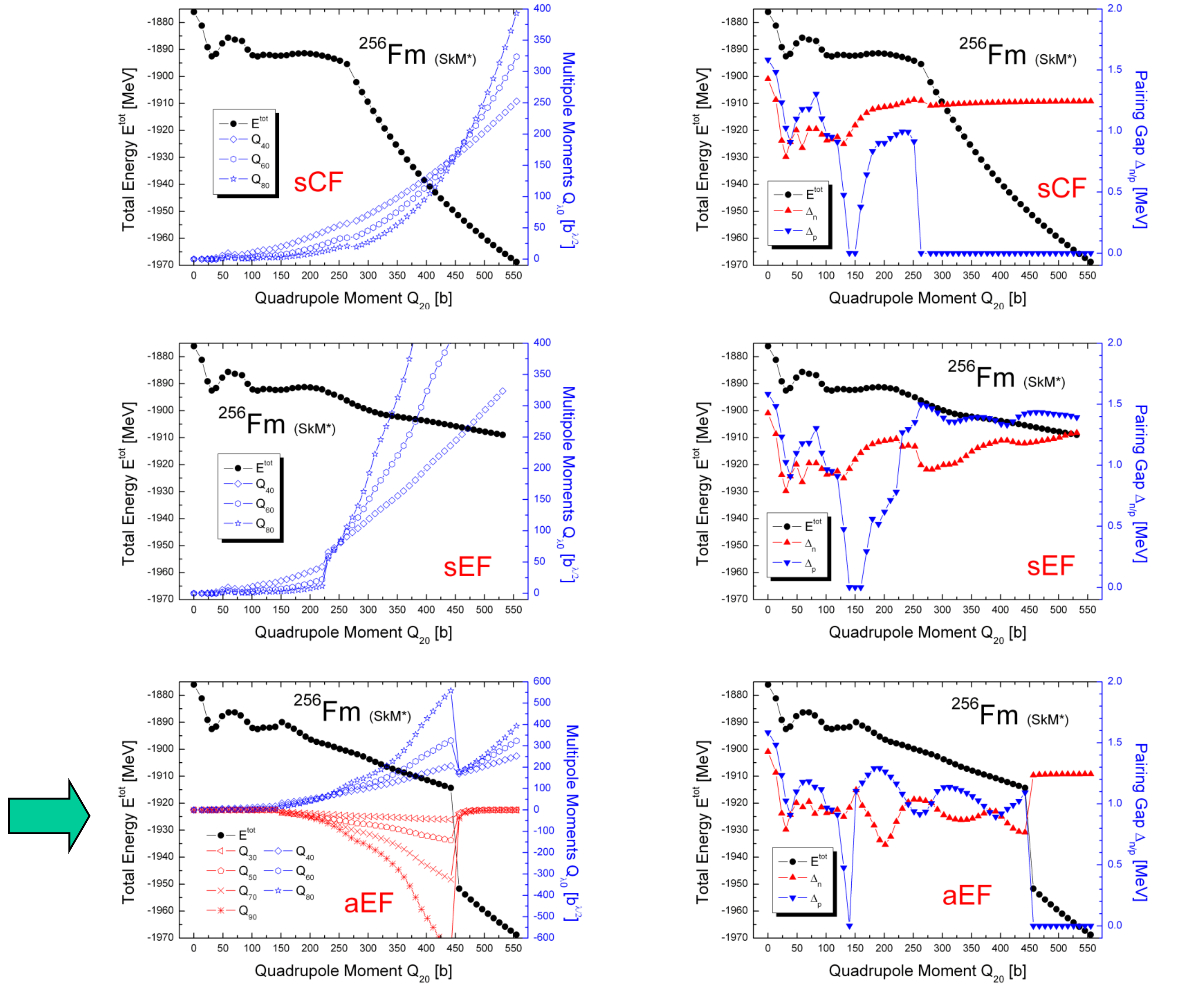

^{256}Fm (SkM*)
sCF
sEF
aEF
Total Energy E^{tot} [MeV]
Quadrupole Moment Q_{20} [b]
Multipole Moments $Q_{\lambda 0}$ [$b^{\lambda/2}$]
Pairing Gap $\Delta_{n/p}$ [MeV]
E^{tot}
Q_{30}
Q_{40}
Q_{50}
Q_{60}
Q_{70}
Q_{80}
Q_{90}
Δ_n
Δ_p

^{256}Fm

“*asymmetric*” fission
(aEF)

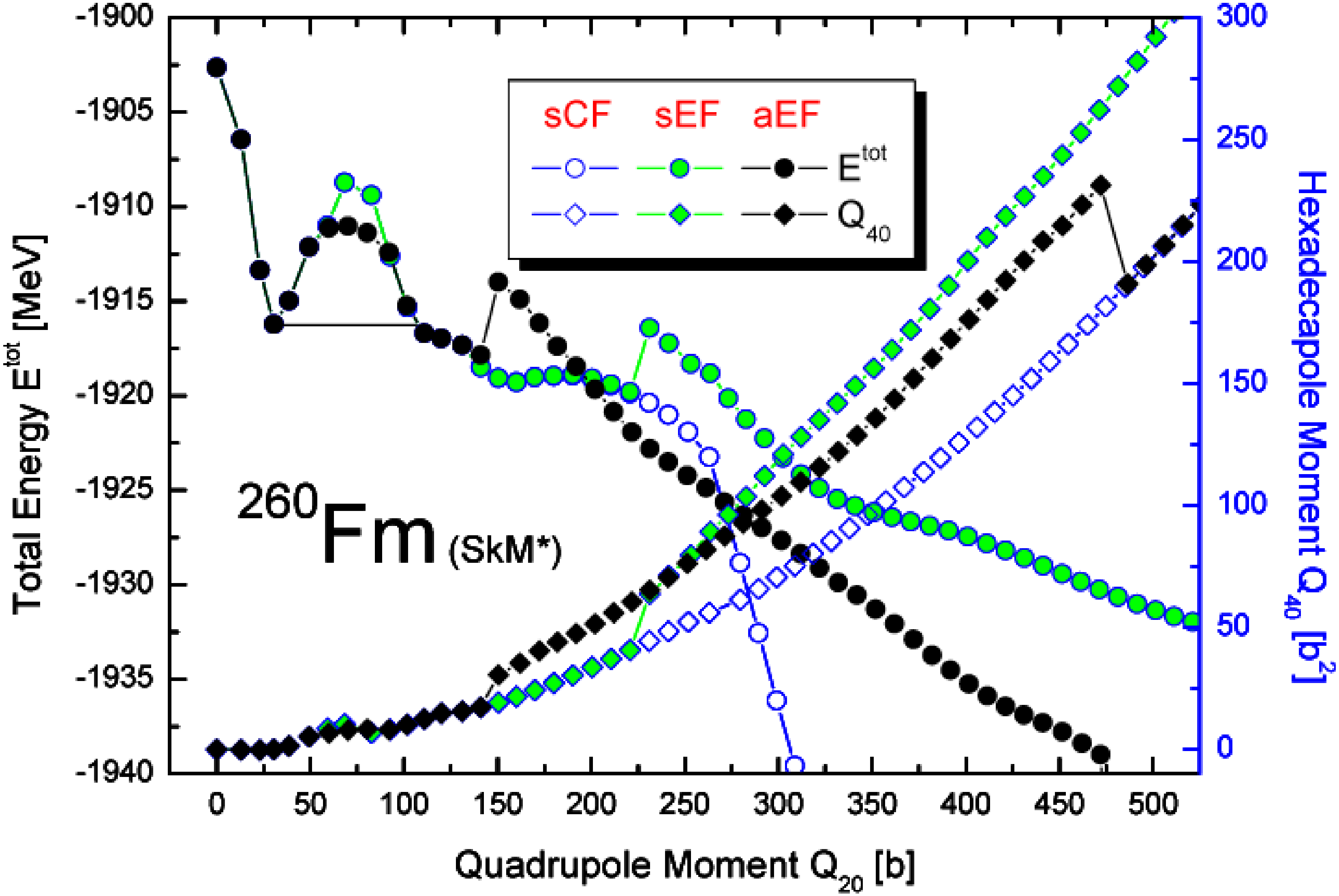

sCF sEF aEF
E^tot
Q40
260Fm (SkM*)
Total Energy E^tot [MeV]
Hexadecapole Moment Q40 [b^2]
Quadrupole Moment Q20 [b]
-1900
-1905
-1910
-1915
-1920
-1925
-1930
-1935
-1940
0 50 100 150 200 250 300 350 400 450 500
300 250 200 150 100 50 0

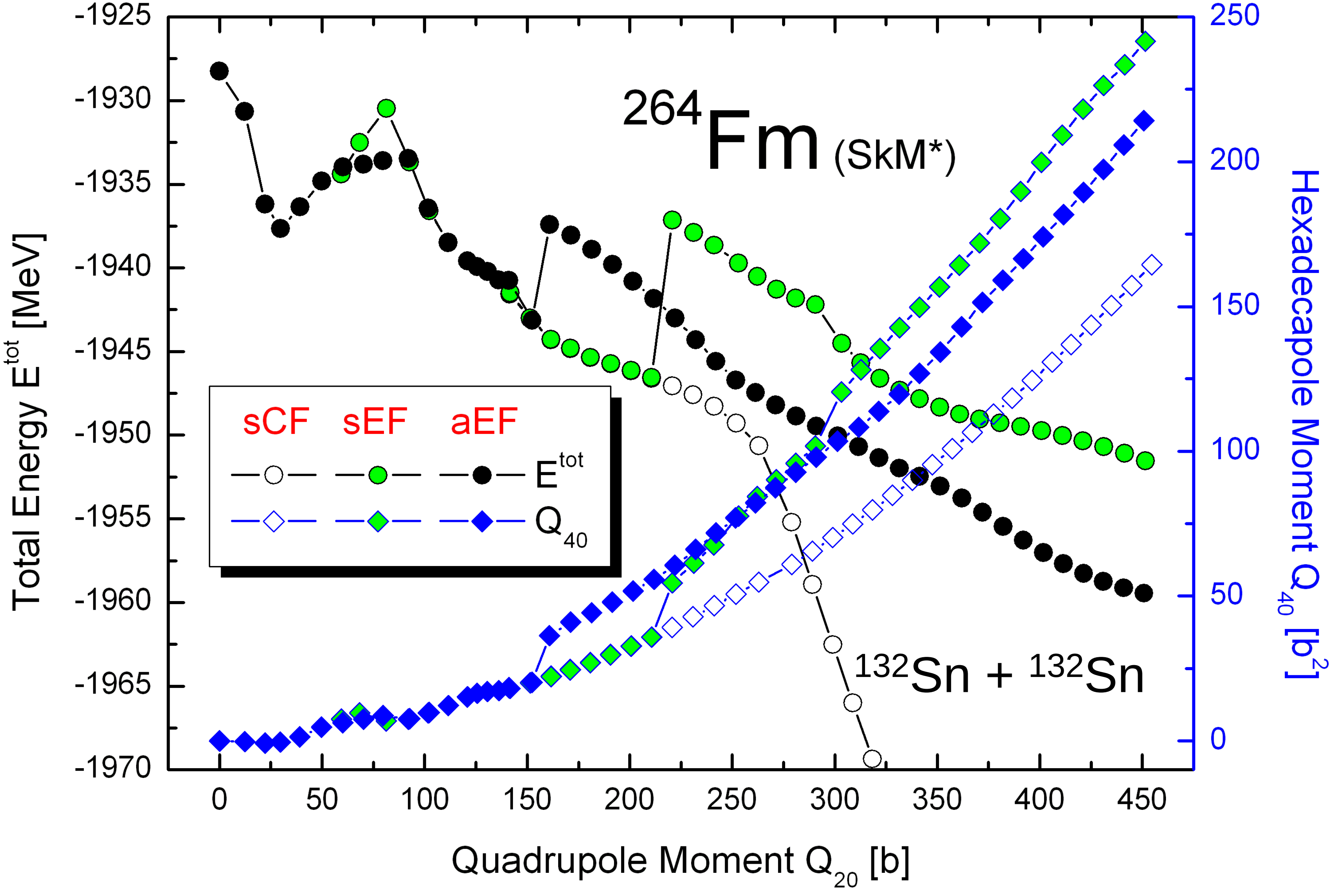

^{264}Fm (SkM*)
^{132}Sn + ^{132}Sn
sCF
sEF
aEF
E^{tot}
Q_{40}
Total Energy E^{tot} [MeV]
Hexadecapole Moment Q_{40} [b^2]
Quadrupole Moment Q_{20} [b]

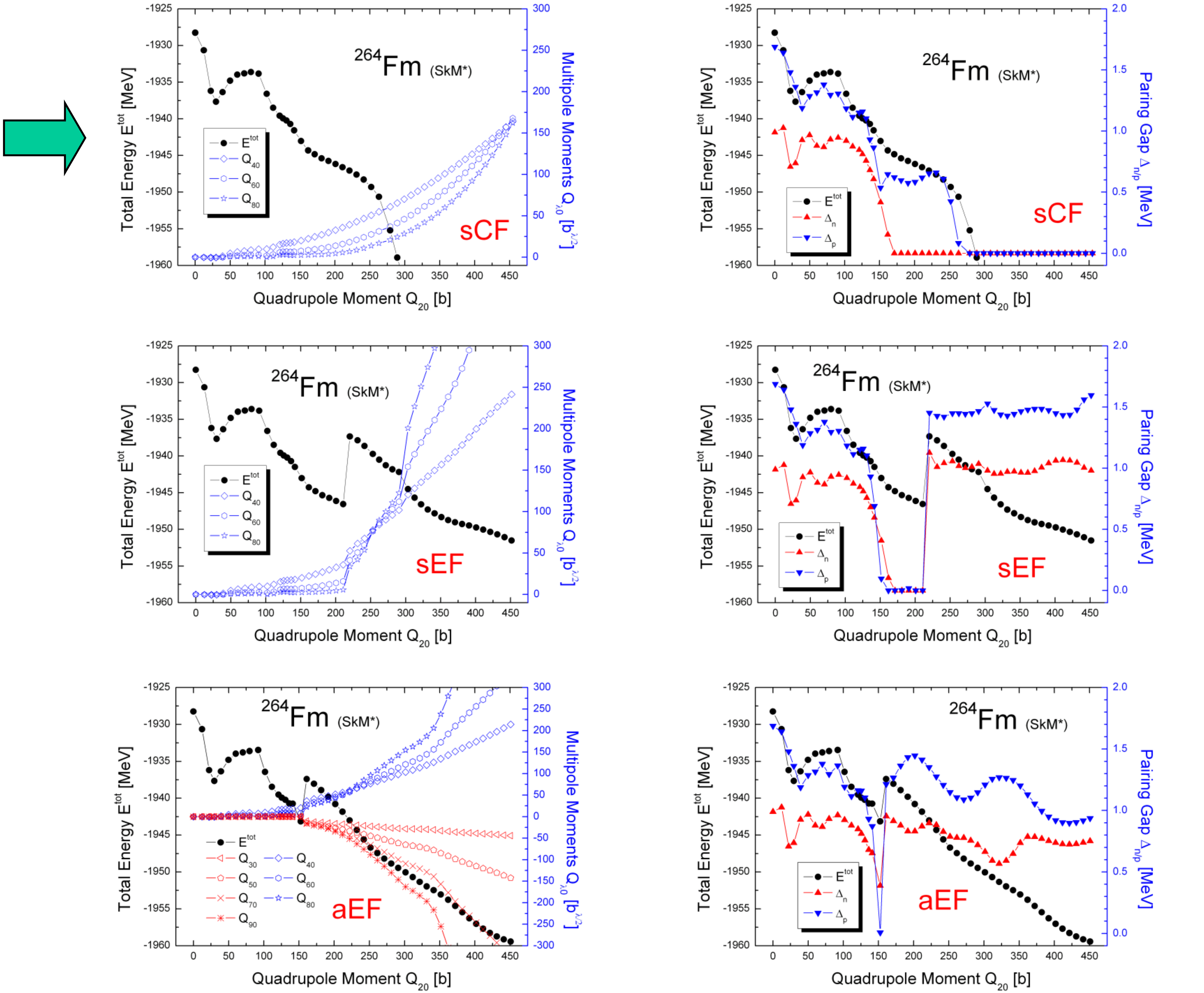

264Fm (SkM*)
sCF
sEF
aEF
Total Energy E^tot [MeV]
Multipole Moments Q_λ0 [b^λ/2]
Paring Gap Δ_n/p [MeV]
Quadrupole Moment Q20 [b]
E^tot
Q30
Q40
Q50
Q60
Q70
Q80
Q90
Δn
Δp

$^{260,264}Fm$

"symmetric-compact"
fission
(sCF)

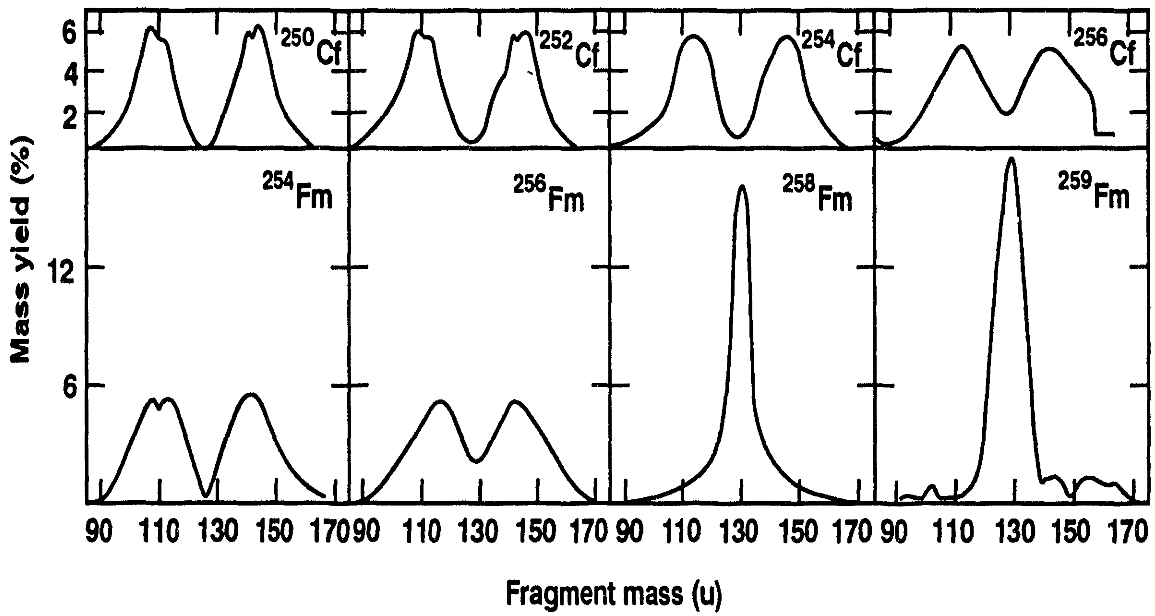

Fig. 2 Mass distributions of the fragments obtained in the spontaneous fission of the Cf and Fm isotopes. Until ^{258}Fm is reached, only slight differences are found in the asymmetrical mass distributions. An abrupt transformation to sharply symmetrical mass distributions occurs at ^{258}Fm.

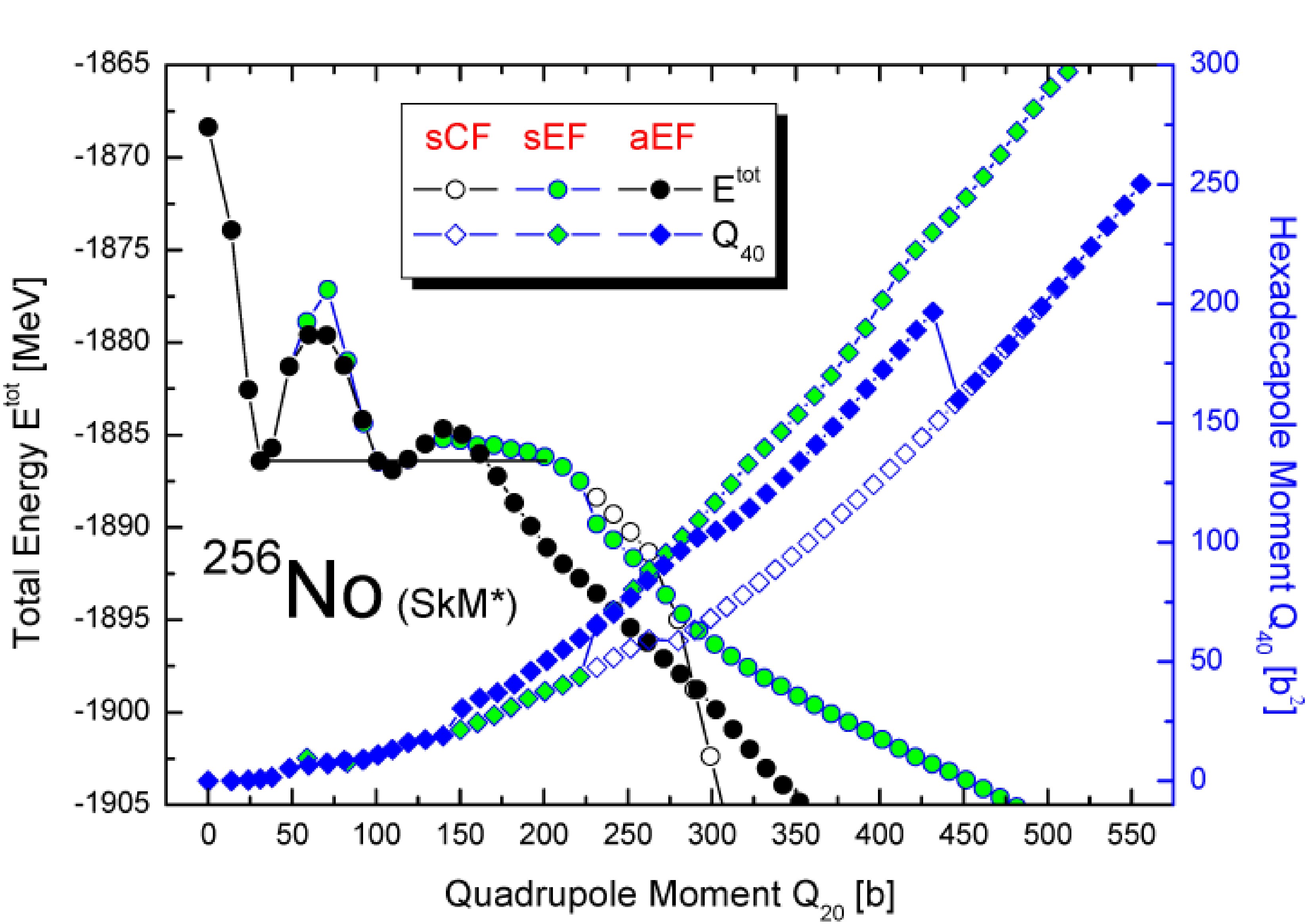

sCF sEF aEF
E^tot
Q_40
256No (SkM*)
Total Energy E^tot [MeV]
Hexadecapole Moment Q_40 [b^2]
Quadrupole Moment Q_20 [b]
-1865
-1870
-1875
-1880
-1885
-1890
-1895
-1900
-1905
0
50
100
150
200
250
300
350
400
450
500
550

^{256}No

"asymmetric" fission (aEF)

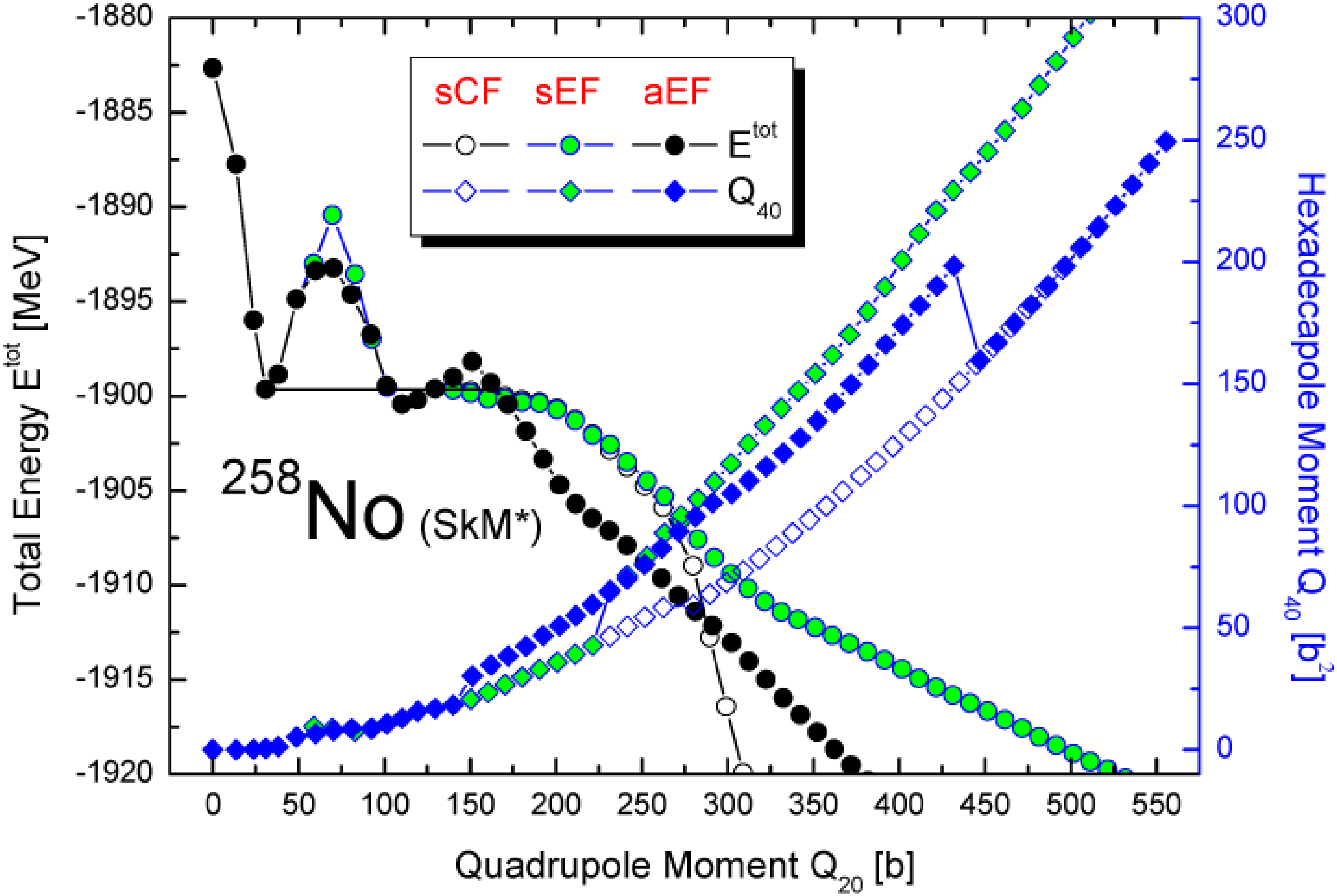

sCF
sEF
aEF
E^tot
Q40
258No (SkM*)
Total Energy E^tot [MeV]
Quadrupole Moment Q20 [b]
Hexadecapole Moment Q40 [b^2]
-1880
-1885
-1890
-1895
-1900
-1905
-1910
-1915
-1920
0
50
100
150
200
250
300
350
400
450
500
550
300
250
200
150
100
50
0

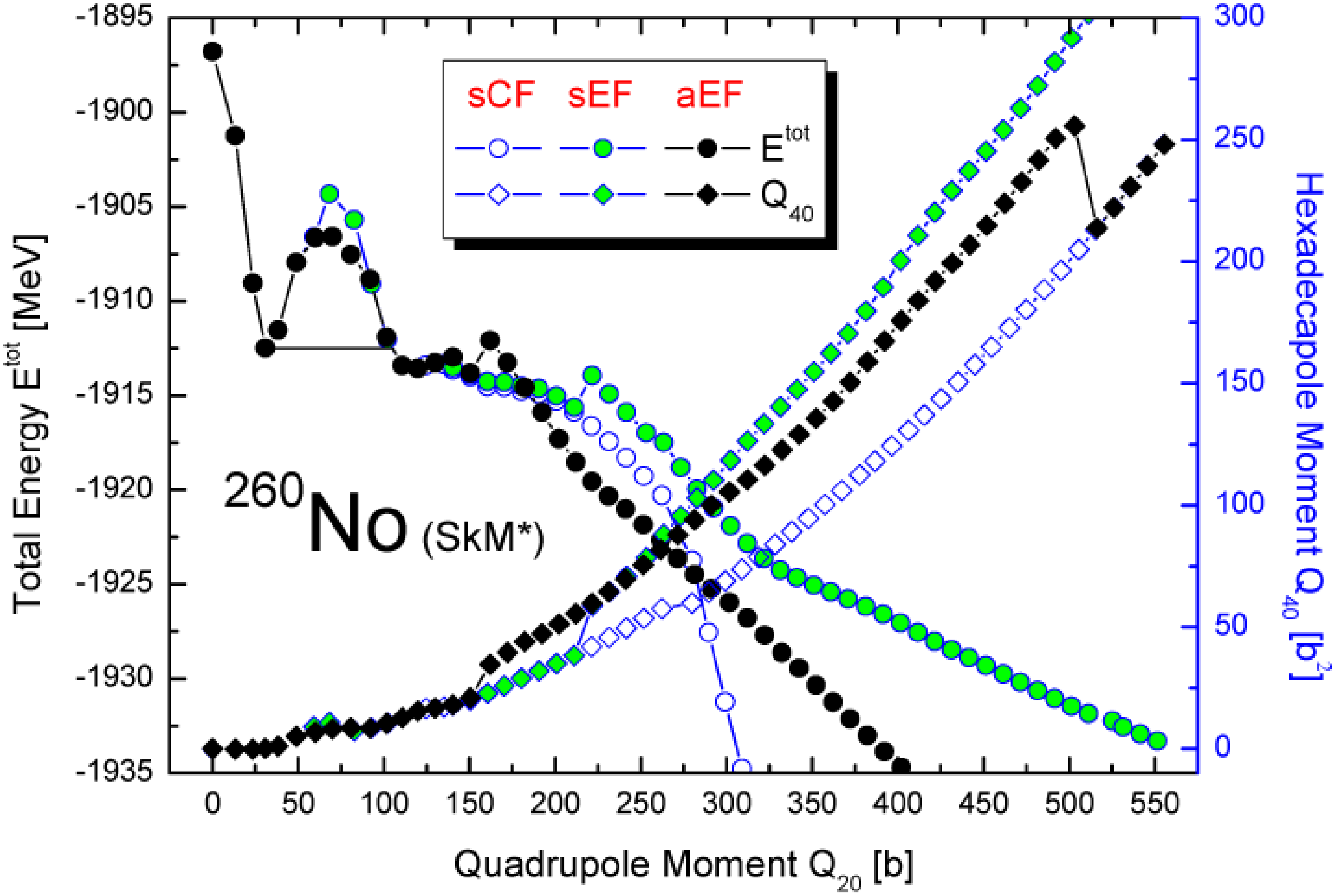

sCF sEF aEF
E^tot
Q40
260No (SkM*)
Total Energy E^tot [MeV]
Hexadecapole Moment Q40 [b^2]
Quadrupole Moment Q20 [b]
-1895
-1900
-1905
-1910
-1915
-1920
-1925
-1930
-1935
0 50 100 150 200 250 300 350 400 450 500 550
300
250
200
150
100
50
0

$^{258,260}No$

"*triple-mod*" fission (sCF, sEF & aEF)

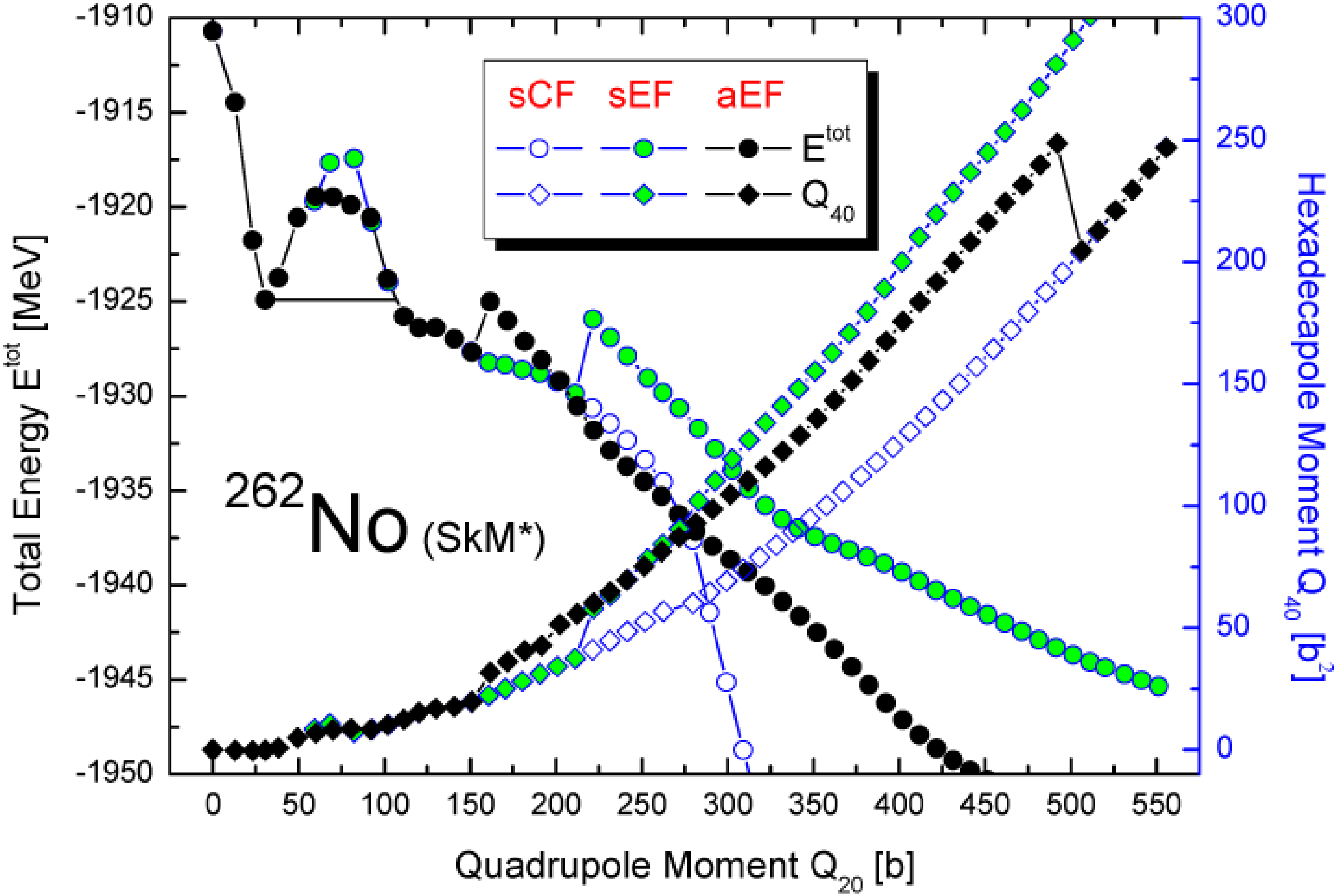

sCF
sEF
aEF
E^tot
Q40
262No (SkM*)
Total Energy E^tot [MeV]
Hexadecapole Moment Q40 [b^2]
Quadrupole Moment Q20 [b]
-1910
-1915
-1920
-1925
-1930
-1935
-1940
-1945
-1950
0
50
100
150
200
250
300
350
400
450
500
550
300
250
200
150
100
50
0

^{262}No

"symmetric-compact"
fission
(sCF)

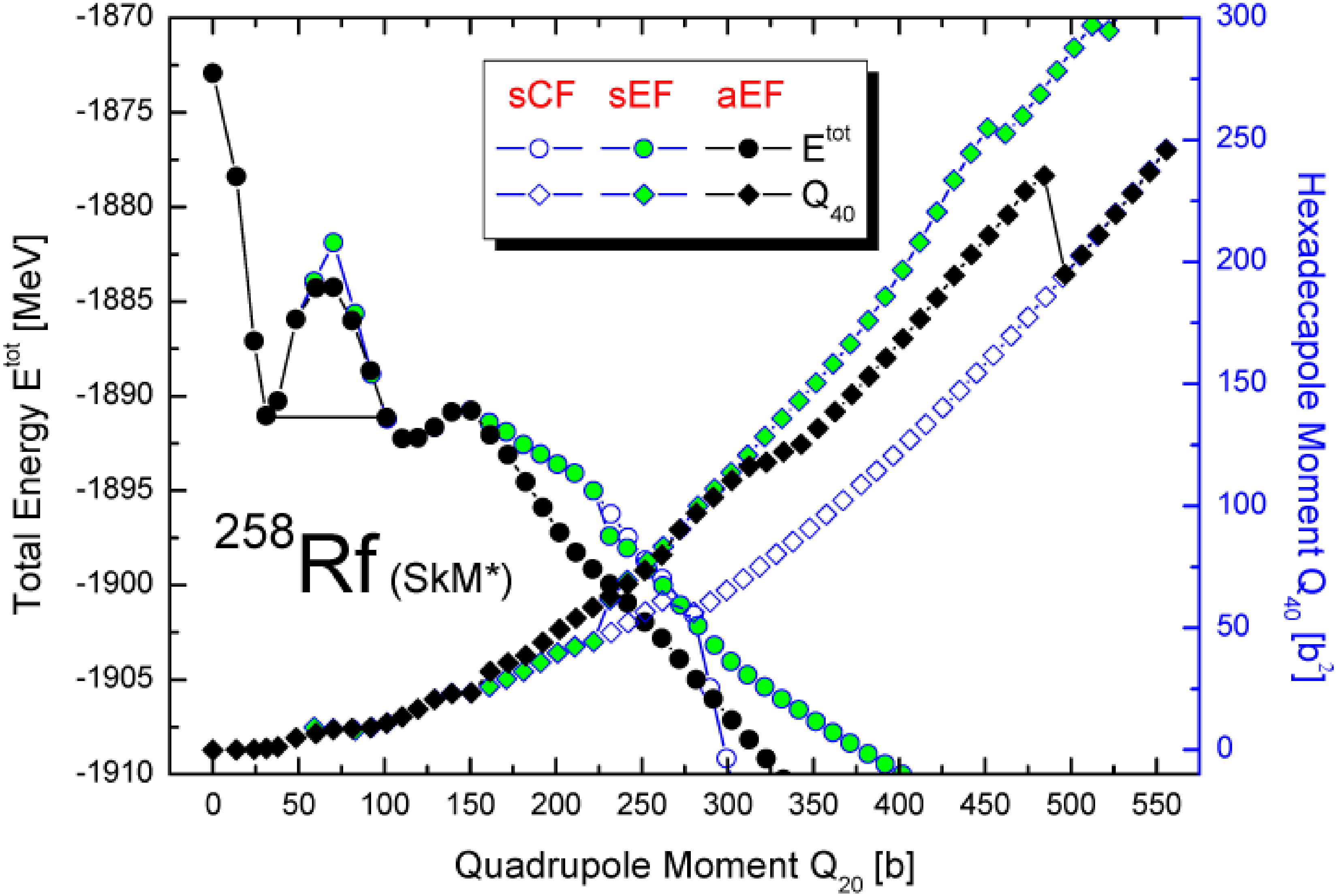

sCF sEF aEF
E^tot
Q_40
258Rf (SkM*)
Total Energy E^tot [MeV]
Hexadecapole Moment Q_40 [b^2]
Quadrupole Moment Q_20 [b]
-1870
-1875
-1880
-1885
-1890
-1895
-1900
-1905
-1910
0
50
100
150
200
250
300
350
400
450
500
550

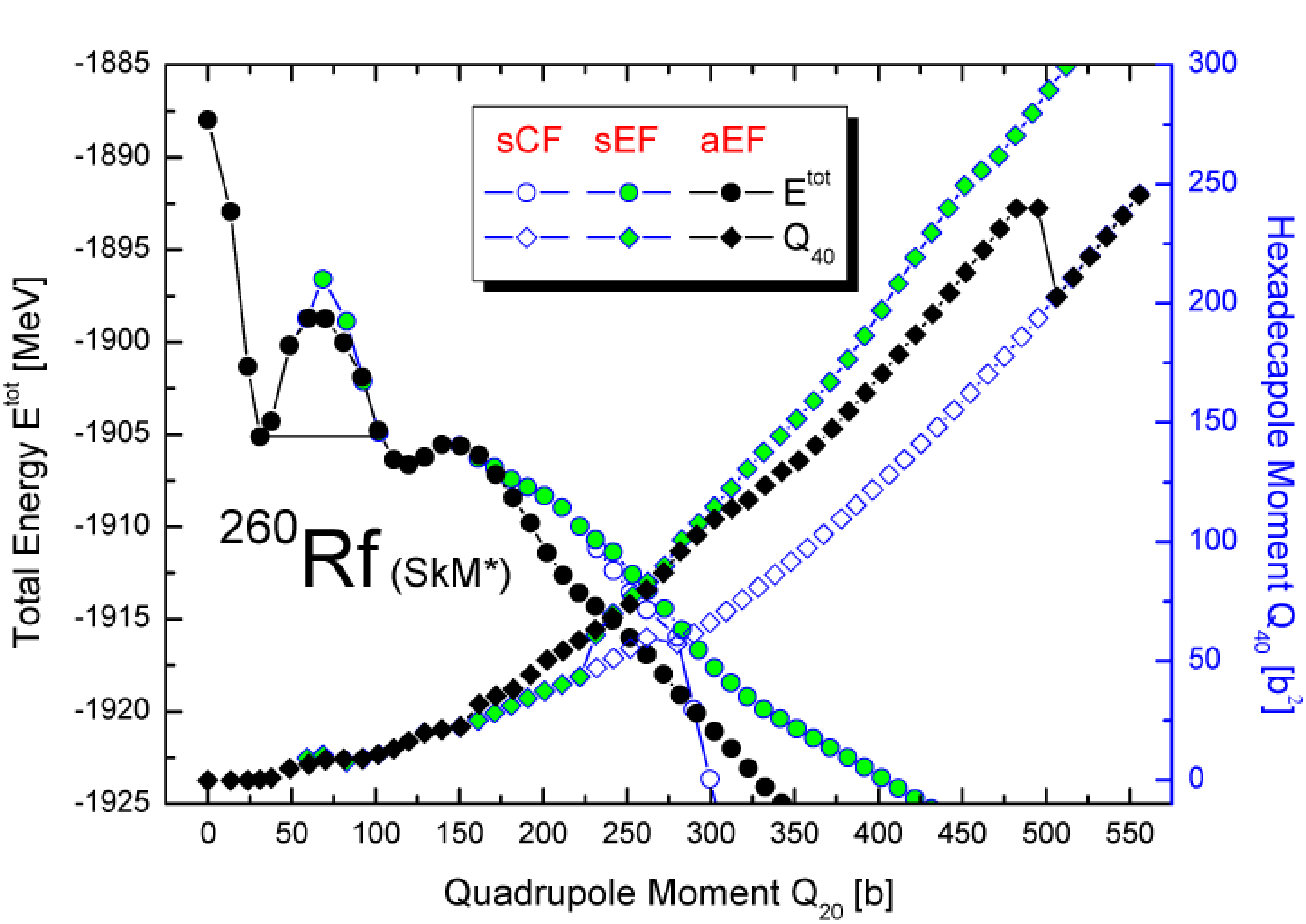

sCF sEF aEF
E^tot
Q40
260Rf (SkM*)
Total Energy E^tot [MeV]
Hexadecapole Moment Q40 [b^2]
Quadrupole Moment Q20 [b]
-1885
-1890
-1895
-1900
-1905
-1910
-1915
-1920
-1925
0 50 100 150 200 250 300 350 400 450 500 550
300
250
200
150
100
50
0

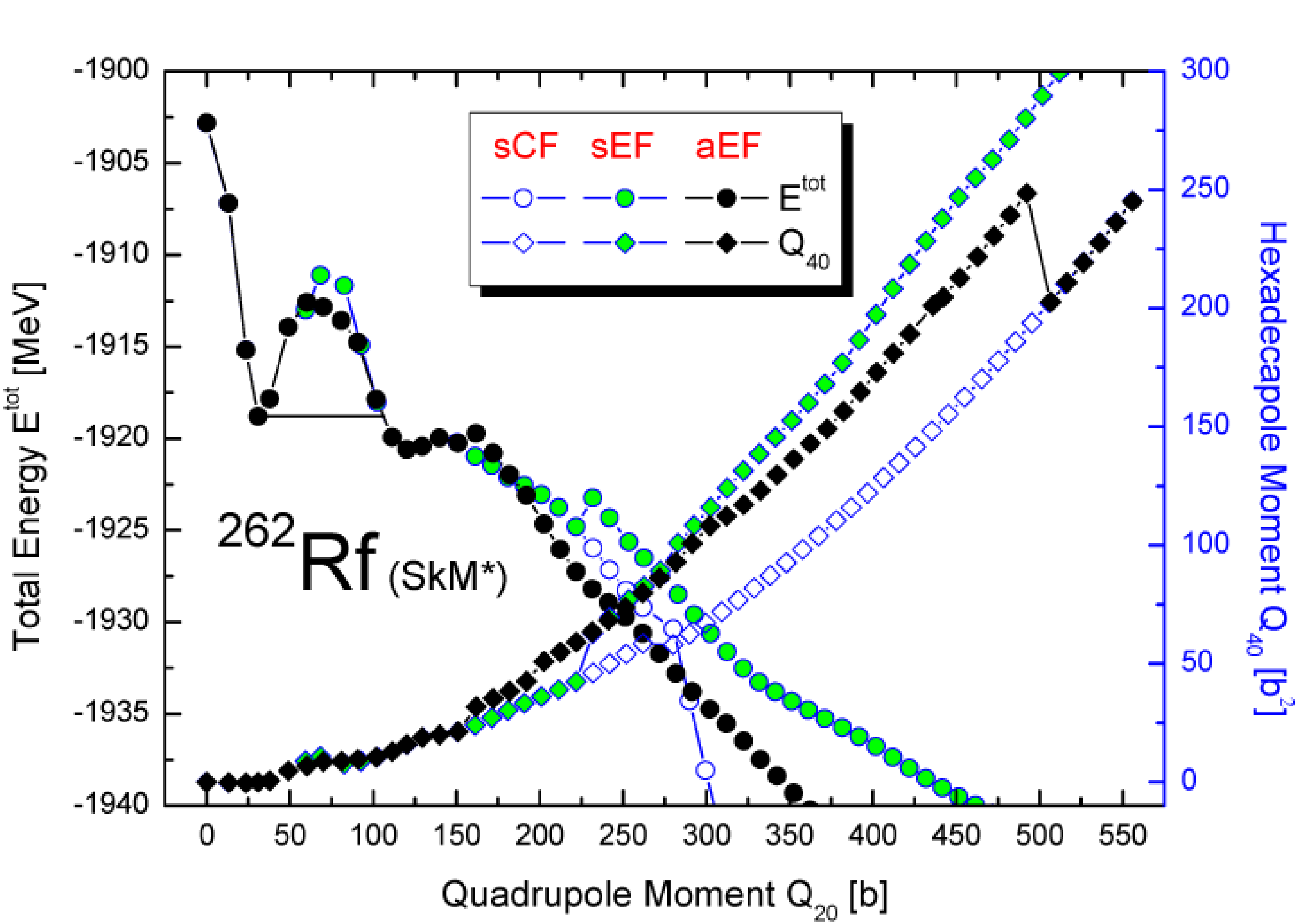

sCF sEF aEF
E^{tot}
Q_{40}
^{262}Rf (SkM*)
Total Energy E^{tot} [MeV]
Hexadecapole Moment Q_{40} [b^2]
Quadrupole Moment Q_{20} [b]
-1900
-1905
-1910
-1915
-1920
-1925
-1930
-1935
-1940
0 50 100 150 200 250 300 350 400 450 500 550
300
250
200
150
100
50
0

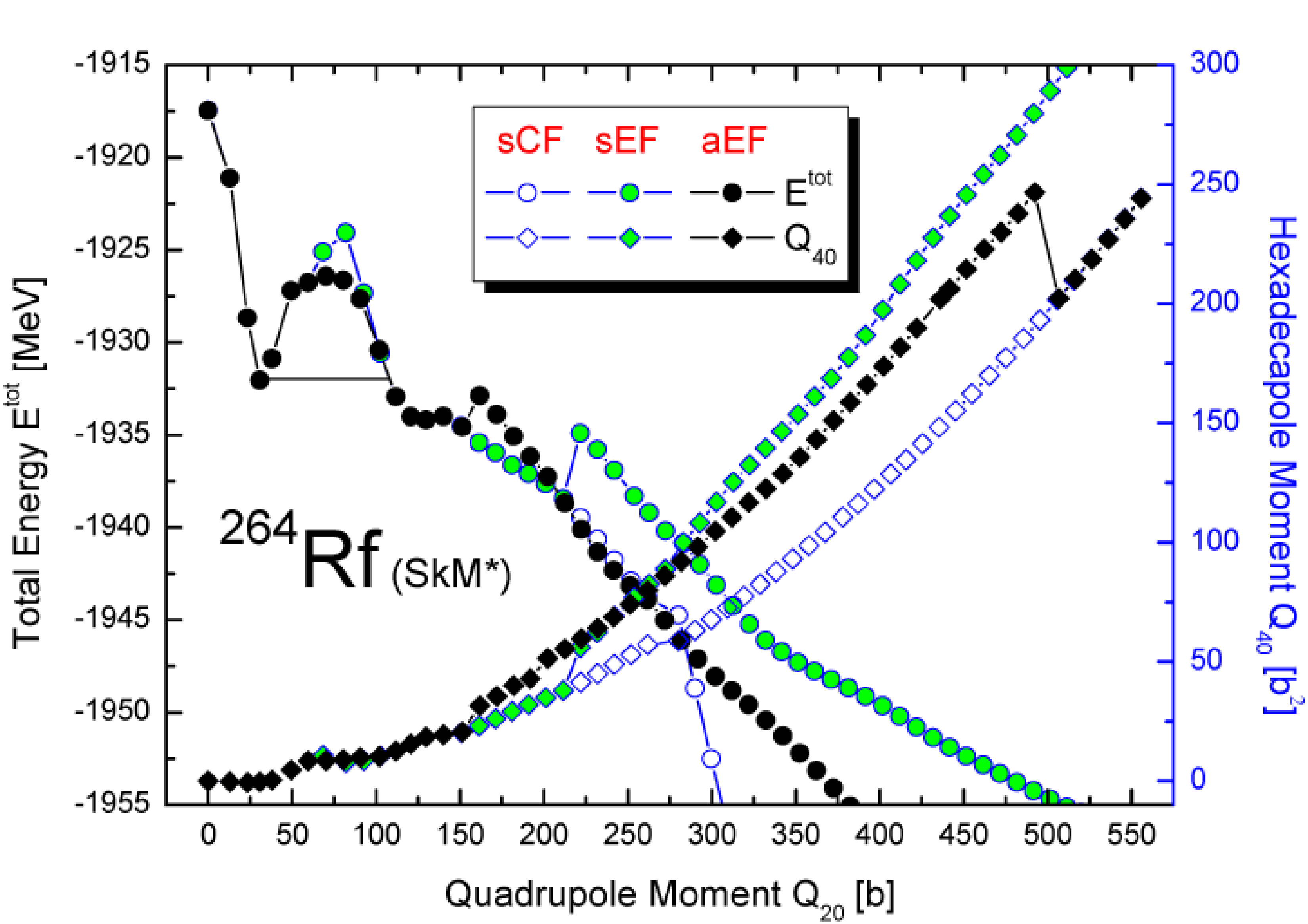

sCF
sEF
aEF
E^tot
Q40
264Rf (SkM*)
Total Energy E^tot [MeV]
Hexadecapole Moment Q40 [b^2]
Quadrupole Moment Q20 [b]
-1915
-1920
-1925
-1930
-1935
-1940
-1945
-1950
-1955
0
50
100
150
200
250
300
350
400
450
500
550

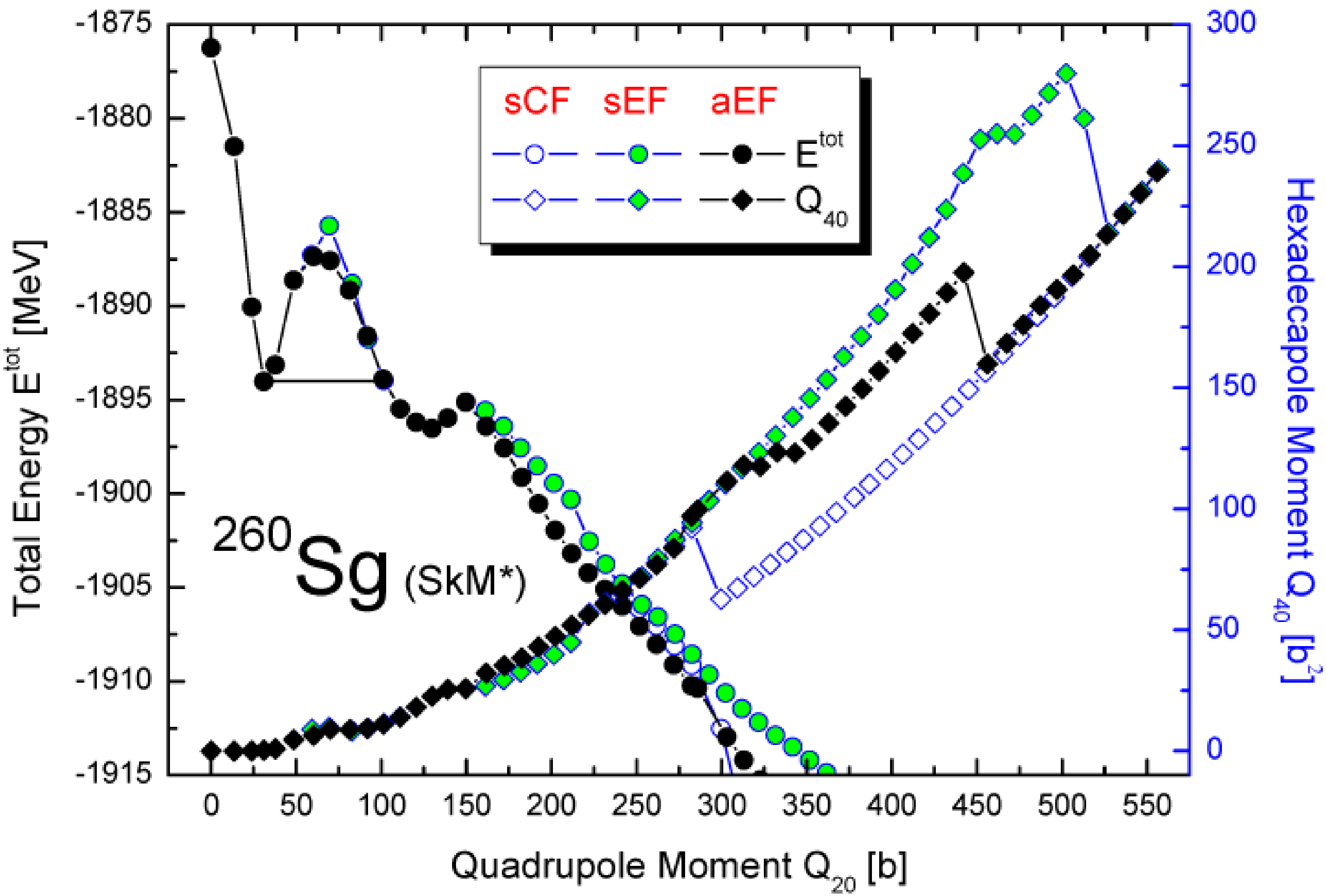

sCF sEF aEF
E^{tot}
Q_{40}
^{260}Sg (SkM*)
Total Energy E^{tot} [MeV]
Quadrupole Moment Q_{20} [b]
Hexadecapole Moment Q_{40} [b^2]
-1875
-1880
-1885
-1890
-1895
-1900
-1905
-1910
-1915
0 50 100 150 200 250 300 350 400 450 500 550
300
250
200
150
100
50
0

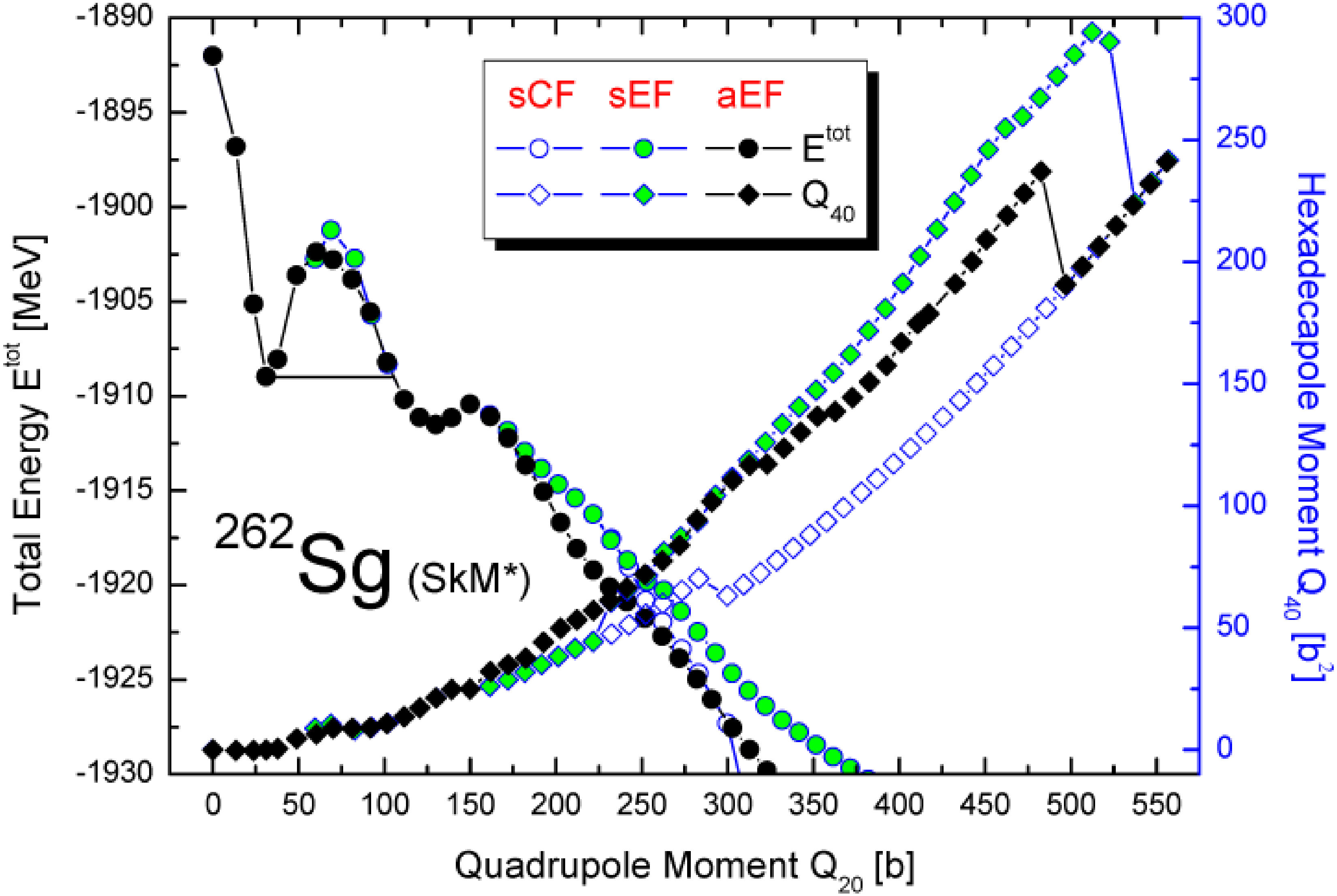

sCF
sEF
aEF
E^tot
Q_40
262Sg (SkM*)
Total Energy E^tot [MeV]
Hexadecapole Moment Q_40 [b^2]
Quadrupole Moment Q_20 [b]
-1890
-1895
-1900
-1905
-1910
-1915
-1920
-1925
-1930
0
50
100
150
200
250
300
350
400
450
500
550

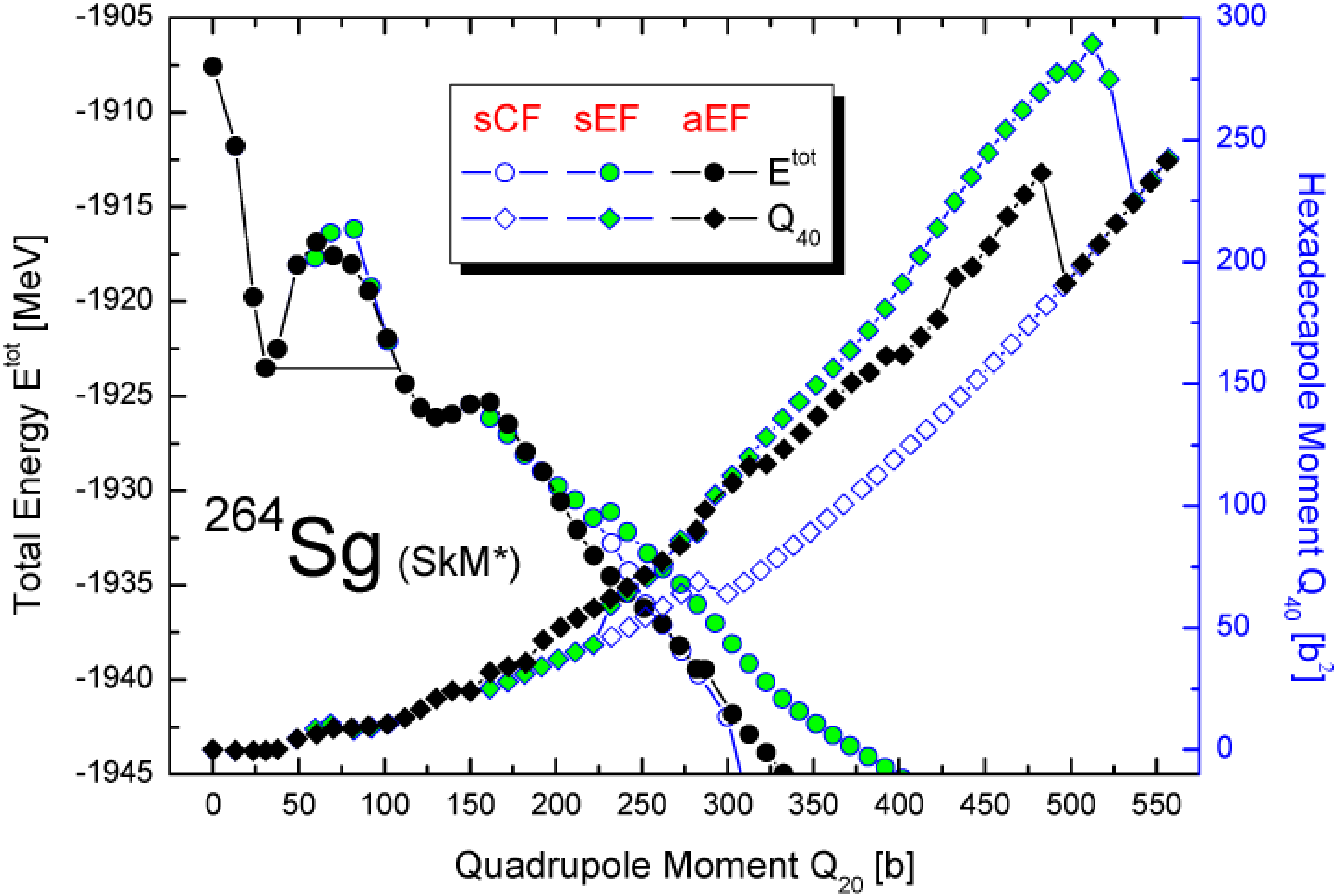

sCF
sEF
aEF
E^tot
Q40
264Sg (SkM*)
Total Energy E^tot [MeV]
Hexadecapole Moment Q40 [b^2]
Quadrupole Moment Q20 [b]
-1905
-1910
-1915
-1920
-1925
-1930
-1935
-1940
-1945
0
50
100
150
200
250
300
350
400
450
500
550
300
250
200
150
100
50
0

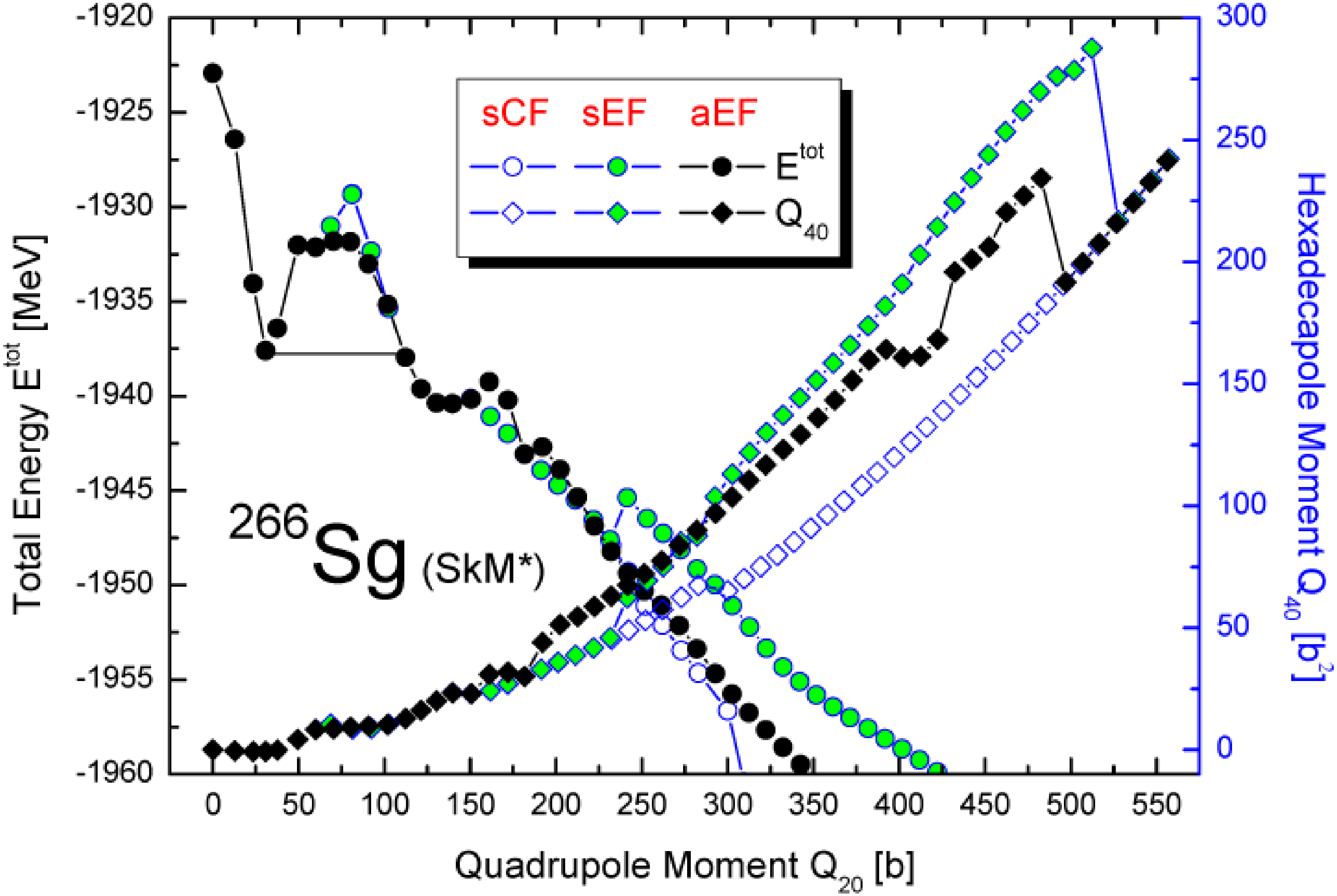

sCF sEF aEF
E^tot
Q40
266Sg (SkM*)
Total Energy E^tot [MeV]
Hexadecapole Moment Q40 [b^2]
Quadrupole Moment Q20 [b]
-1920
-1925
-1930
-1935
-1940
-1945
-1950
-1955
-1960
0
50
100
150
200
250
300
350
400
450
500
550

KONIEC